General Disclaimer

One or more of the Following Statements may affect this Document

- This document has been reproduced from the best copy furnished by the organizational source. It is being released in the interest of making available as much information as possible.

- This document may contain data, which exceeds the sheet parameters. It was furnished in this condition by the organizational source and is the best copy available.

- This document may contain tone-on-tone or color graphs, charts and/or pictures, which have been reproduced in black and white.

- This document is paginated as submitted by the original source.

- Portions of this document are not fully legible due to the historical nature of some of the material. However, it is the best reproduction available from the original submission.

NASA

Technical Memorandum 79689

A Hydrological Analysis of East Australian Floods Using Nimbus-5 Electrically Scanning Microwave Radiometer Data

Lewis J. Allison, Thomas J. Schmugge and Gavin Byrne

MARCH 1979

A HYDROLOGICAL ANALYSIS OF EAST AUSTRALIAN FLOODS USING

NIMBUS-5 ELECTRICALLY SCANNING MICROWAVE RADIOMETER DATA
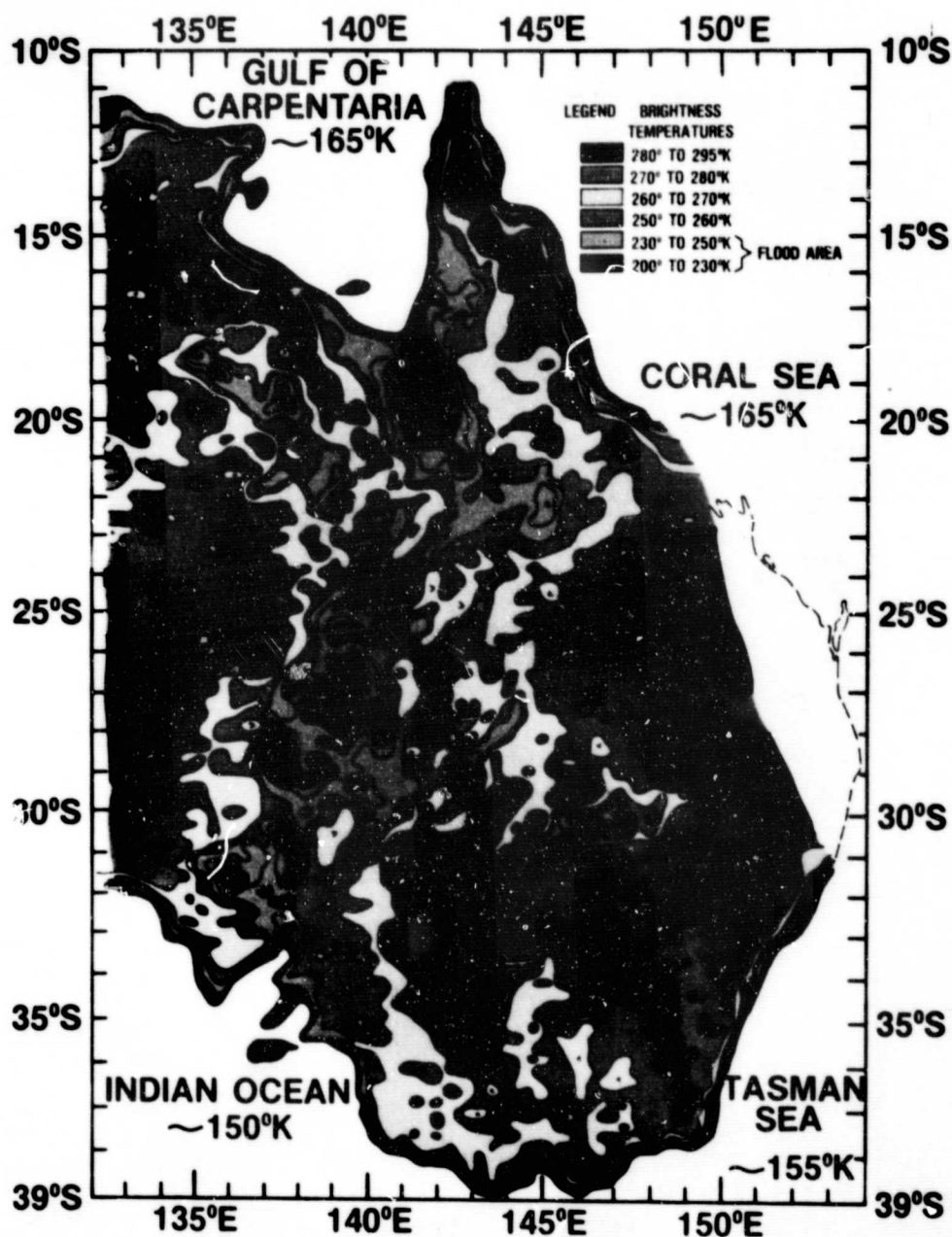
Lewis J. Allison
Thomas J. Schmugge
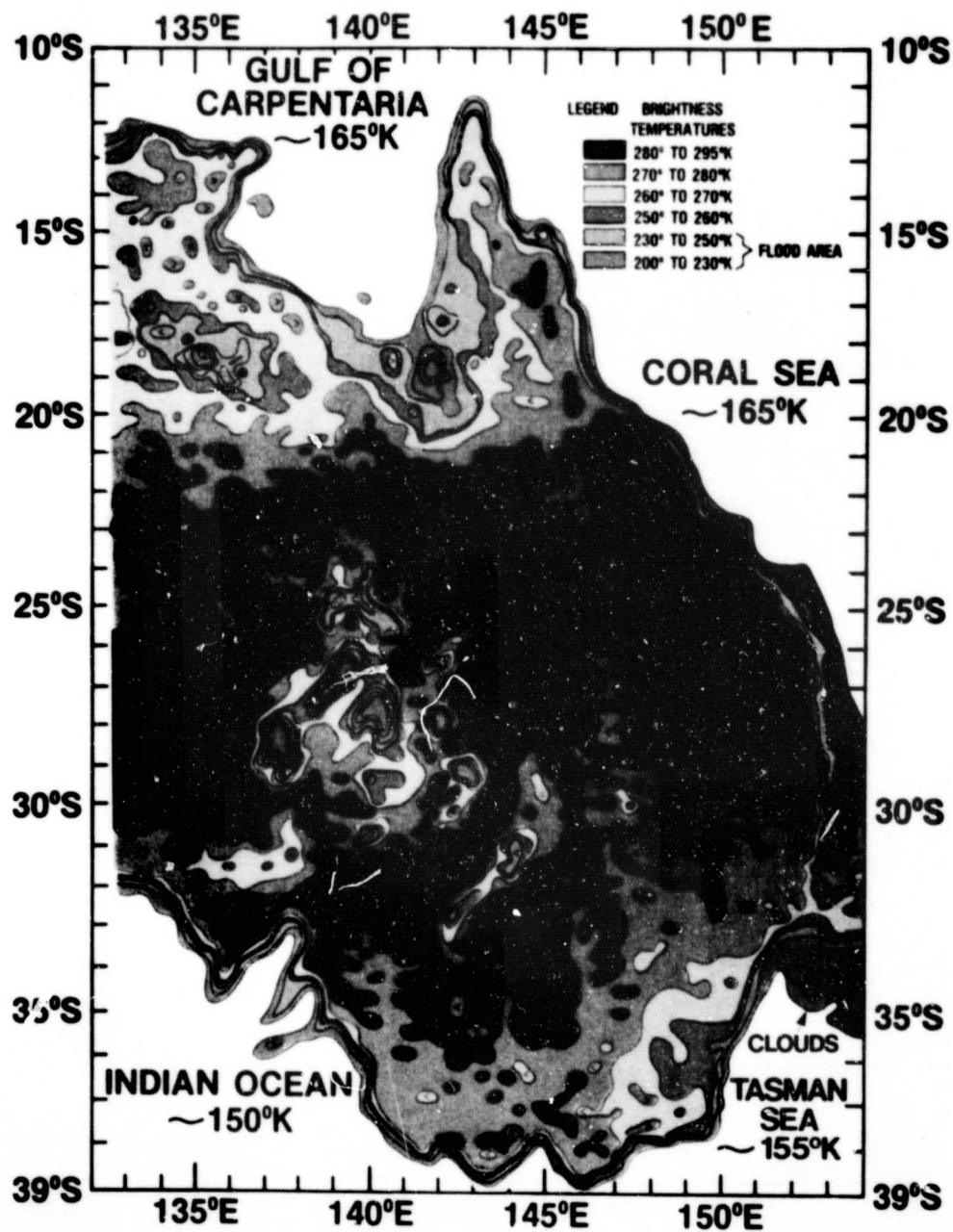
Goddard Space Flight Center
Greenbelt, Maryland 20771

Gavin Byrne
Commonwealth Scientific and Industrial Research Organization (CSIRO)
Canberra, A. C. T., Australia

GODDARD SPACE FLIGHT CENTER
Greenbelt, Maryland

Frontispiece 1. East Australian floods as revealed by day by Nimbus-5 Electrically Scanning Microwave Radiometer (19.35 GH$_z$) on 1 February 1974 (maximum extent). Blue (250° to 230°K) and purple (230° to 200°K) brightness values indicate flooded surfaces in good agreement with aircraft photos, hydrological data and Landsat imagery.

Frontispiece 2. East Australian floods as revealed by day by Nimbus-5 Electrically Scanning Microwave Radiometer (19.35 GH$_z$) on 11 March 1974 (near minimum extent). Blue (250° to 230°K) and purple (230° to 200°K) brightness values indicate flooded surfaces.

A HYDROLOGICAL ANALYSIS OF EAST AUSTRALIAN FLOODS USING NIMBUS 5 ELECTRICALLY SCANNING MICROWAVE RADIOMETER DATA

Lewis J. Allison
Thomas J. Schmugge

Goddard Space Flight Center
Greenbelt, Maryland 20771

Gavin Byrne
Commonwealth Scientific and Industrial Research Organization (CSIRO)
Canberra, A.C.T., Australia

ABSTRACT

The chronological development and diminution of six floods in eastern Australia during January, February and March 1974 were mapped for the first time by the Nimbus Electrically Scanning Microwave Radiometer (ESMR). Day and nighttime ESMR (19.35 GH_z) coverage was analyzed for the low gradient, flooded Darling River system in New South Wales. Apparent movement of surface water as indicated by low brightness temperatures ($<250°K$, day and $<240°K$, night) was easily followed around the curved runoff basin along the northern shoreline of the flooded Darling River during this 3-month period. This pattern was in good agreement with flood crest data at selected river height gage stations, even under cloudy conditions.

CONTENTS

ILLUSTRATIONS

Frontispiece 1. East Australian floods as revealed by day by Nimbus-5 Electrically Scanning Microwave Radiometer (19.35 GH_z) on 1 February 1974 (maximum extent). Blue (250° to 230°K) and purple (230° to 200°K) brightness values indicate flooded surfaces in good agreement with aircraft photos, hydrological data and Landsat imagery.

Frontispiece 2. East Australian floods as revealed by day by Nimbus-5 Electrically Scanning Microwave Radiometer (19.35 GH_z) on 11 March 1974 (near minimum extent). Blue (250° to 230°K) and purple (230° to 200°K) brightness values indicate flooded surfaces.

ILLUSTRATIONS (Continued)

A HYDROLOGICAL ANALYSIS OF EAST AUSTRALIAN FLOODS USING
NIMBUS 5 ELECTRICALLY SCANNING MICROWAVE RADIOMETER DATA

1. INTRODUCTION

The Nimbus-5, a research and development satellite launched on December 12, 1972, carried the electrically-scanning microwave radiometer (ESMR) which recorded microwave brightness temperatures (T_B) from which it has been possible to estimate meteorological and hydrological parameters on a global scale.

The microwave brightness temperature (T_B) of the Earth's surface is essentially the product of the surface temperature and surface emissivity with additional attenuation and emissions due to atmospheric water vapor and liquid water droplets (Allison et al., 1975, Zwally and Gloersen, 1977). Ice crystal clouds (Cirrus) have little effect on microwave radiation and are essentially transparent at the 1.55cm ESMR wavelength. Molecular oxygen absorption can also be neglected at this wavelength (Wilheit et al., 1977). Emissivity is the ratio of the radiation from a surface at a measurable temperature for a given wavelength interval to that of a black-body source at the identical temperature. When the emissivity is 1, the surface radiates as a black-body. When it is less than 1, the surface behaves as a graybody (Moore et. al., 1975). The emissivity of the surface depends among other things on the medium's dielectric properties and for a smooth surface can range from 0.4 for water which has a large dielectric constant, to about 0.7 for wet soils to greater than 0.9 for dry soils and dense vegetation. Microwave emission from surfaces is also affected by roughness, topographic slope, stratigraphy (layering of different materials), density of rocks and vegetation cover (Oberste-Lehn, 1970, Cihlar and Ulaby, 1974, Vickers and Rose, 1971, Allison, 1977). For example, a smooth bare dry soil surface whose physical temperature was 290°K and emissivity was 0.90 to 0.95, would indicate a T_B of 261° to 275°K. This is to be contrasted to the low T_B values over the calm ocean which is approximately 120°, a result of low water emissivities of ~ 0.4, at 19.35 GH_z.

1

The state of the sea surface (wave height, roughness and foam) would increase the observed brightness temperature for winds above 7 m/sec at the rate of 1°K/m/sec) (Nordberg et al., 1971).

Nimbus-5 ESMR data has been used to detect rainfall over the ocean by Allison et al., 1974, Rao et al., 1976, Kidder and Von der Haar, 1977, Wilheit et al., 1977, Adler and Rodgers, 1977, Austin and Geotis, 1978, Stout and Martin, 1979. This is possible because the oceans provide a relatively constant, low T_B ($\leq$ 150 K) background for observing the atmosphere. Over land the background is warmer, typically above 250°K, and more variable, as a result attempts to measure rainfall over land with the Nimbus 5 ESMR have failed (Meneely, 1975). However there has been some limited success in delineating rain over land using theoretical analysis and actual case studies of the dual polarized Nimbus-6 ESMR (37GH$_z$). (Rodgers et al., 1978, Savage and Weinman, 1975.) The effect of rainfall over the ocean is to increase the T_B observed from space up to 250 or 260 K for high rain rates. The rate of increase in T_B depends on the wavelength. At the 1.55 cm Nimbus 5 ESMR wavelength, this maximum is reached for a rain rate of approximately 10 mm/hr (Wilheit et al., 1977). This relationship has been used to determine rainfall rates over the oceans thus providing information for regions of the earth for which there were very few conventional data available. These data have been combined to produce an atlas of the monthly averages of rainfall over the oceans (Rao and Theon, 1977).

The extent of a disastrous regional flood in the Mississippi Valley at varying recurrence intervals was mapped by use of Landsat (Rango and Anderson, 1974, Rango and Salomonson, 1974, Otterman et al., 1976). NOAA VHRR (Wiesnet et al., 1974) and Nimbus-5 ESMR data (Schmugge et al., 1974 (a)). However a complete time sequence of a major flood had not yet been demonstrated by satellite analysis. This paper will present Nimbus 5 microwave data which were used to detect and map the movement of flooded areas in eastern Australia from January to March 1974.

2.   ELECTRICALLY–SCANNING MICROWAVE RADIOMETER EXPERIMENT

The Nimbus-5 spacecraft (Fig. 1) was flown in a near-polar (81° retrograde) sunsynchronous circular orbit of about 1100km (600 n. mi.). Each orbit crossed the equator northward at approximate local noon and southward at midnight with a 27° longitude separation and a period of 107 minutes. The Nimbus-5 ESMR measures the emitted radiation from the earth's surface and intervening atmosphere in the $250MH_z$ band centered at $19.35 GH_z$ (1.55 cm), with a noise equivalent temperature difference (NEΔT) of approximately 2K. It scans transverse to the flight path every 4 seconds from 50° to the left through nadir to 50° to the right in 78 steps with some overlap. The scanning process is controlled by an onboard computer and the radiometer scans a region whose width is approximately 30° of longitude at 30°N. The half-power beamwidth of the antenna is 1.4° at nadir and the 2.2° at 50° edges with resultant footprints of 22km and 45 by 160km, respectively. Since the ESMR senses horizontally polarized radiation, a scan-angle dependent correction was applied to the data to make each observation more closely equivalent to a linearly polarized nadir observation (Wilheit, 1973). The instrument and its basic physics is discussed in more detail by Wilheit, 1972 Wilheit et al., 1973, Allison et al., 1974.

3
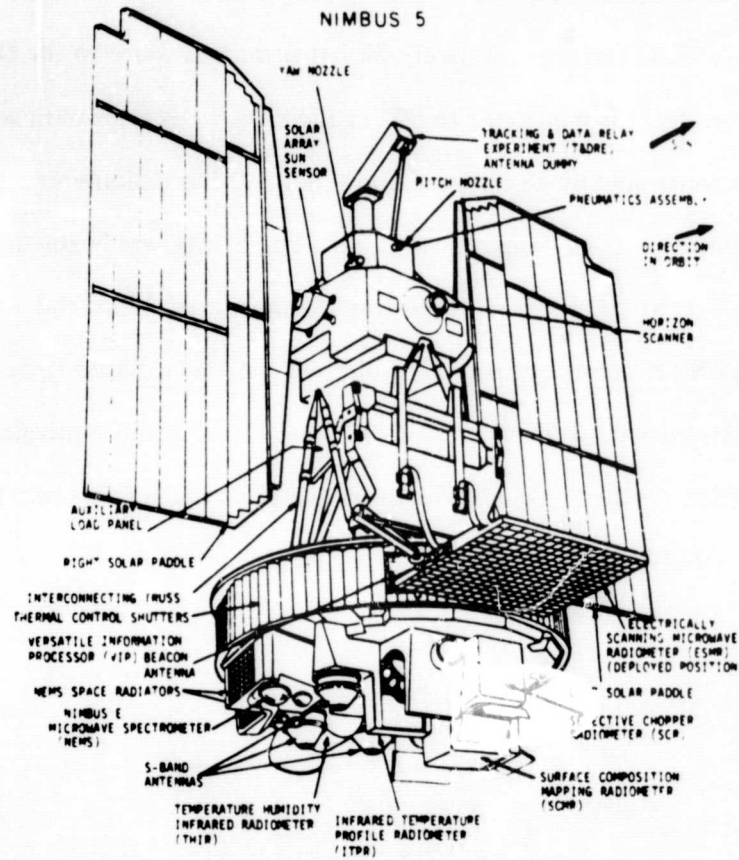
Figure 1. The Nimbus-5 Spacecraft and Associated Experiments

3. MICROWAVE BRIGHTNESS TEMPERATURE VERSUS SOIL MOISTURE MEASUREMENTS

Since the dielectric constant of water can be as large as 80 and dry soil as low as 3, the water content of soil will have a strong effect on the soil's dielectric properties. The resulting emissivity of nonvegetated surfaces has been observed to vary from 0.6 to > 0.95 and, depending on the soil moisture content, the occurrence of dew, the surface temperature, and receiver polarization, can indicate microwave brightness temperatures from < 200° to > 310°K. This range of T_B was observed in ground based experiments (Poe et al., 1971, Newton, 1977), experiments from aircraft (Schmugge et al., 1974 (b) and 1976) and from spacecraft (Eagleman and Lin, 1976).

An example of the aircraft results at 1.55 cm wavelengths are presented in Fig. 2(a to c) where T_B is plotted versus soil moisture. These data were obtained over bare agricultural fields near Phoenix, Arizona and in the Imperial Valley of Southern California during March 1972. It was found that microwave emissivity of heavy soils (high clay content) Fig. 2(b) showed a lesser sensitivity (slope) to soil moisture content than the light soils (sandy loam) Fig. 2(a). The dependence on soil type was removed by expressing soil moisture content in units of percent of field capacity by use of the following empirical equation (Schmugge et. al., 1976).

Field capacity (FC) = 2.51 – 0.21 x Sand + 0.22 x Clay,

where sand and clay represent respective soil fractions in percent. In Figure 2(c) there is a 50-60K variation of T_B between dry and saturated soils. Dry soils are those below about 40 percent field capacity which is approximately the wilting point, and saturated soils are those with moisture levels in excess of 100 percent of field capacity. These aircraft observations indicate the sensitivity of the radiometer operating at 1.55 cm wavelength to soil moisture variations for bare ground situations. When vegetation was present the sensitivity to soil moisture changes was significantly decreased due to the screening effects of the vegetation.
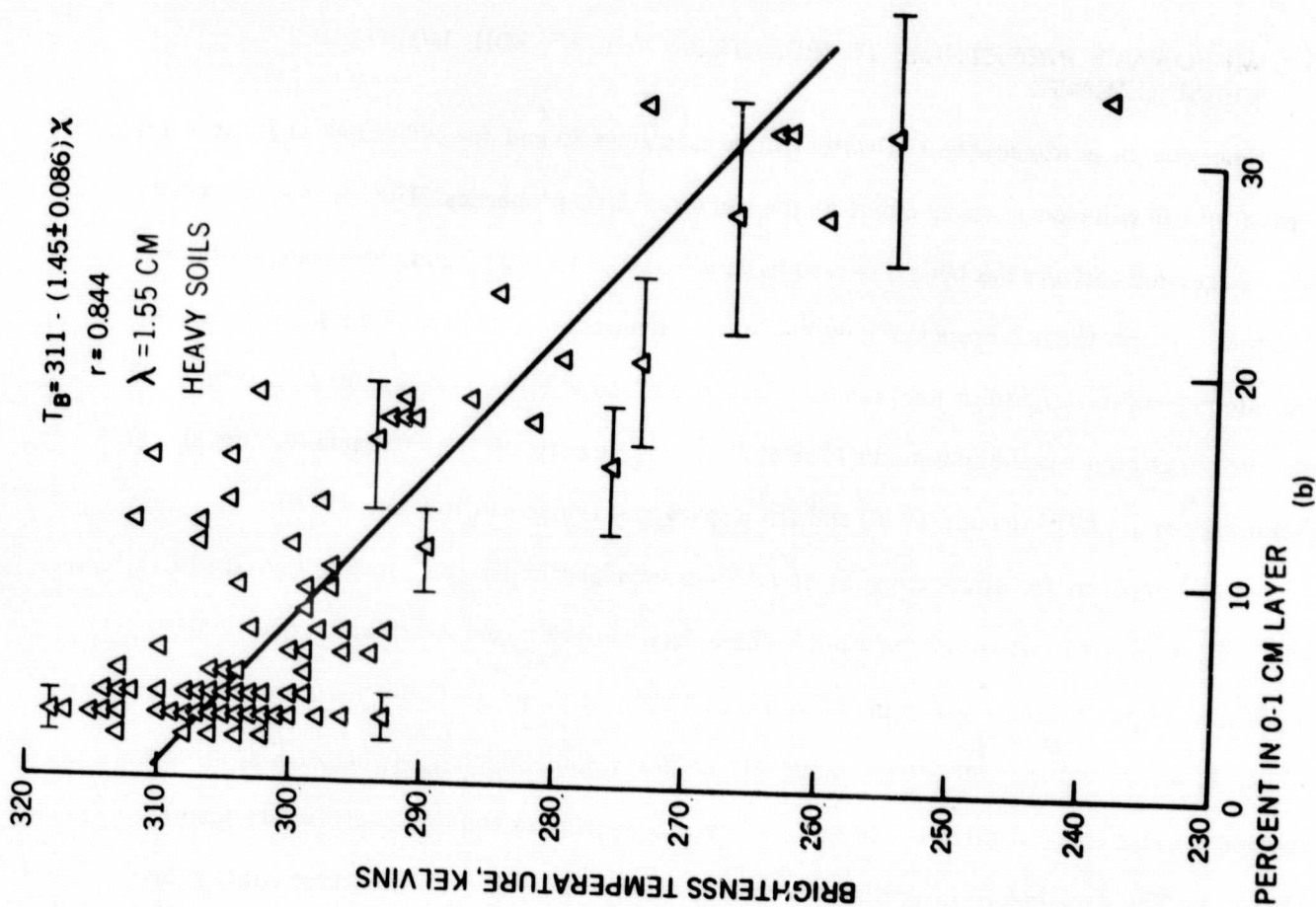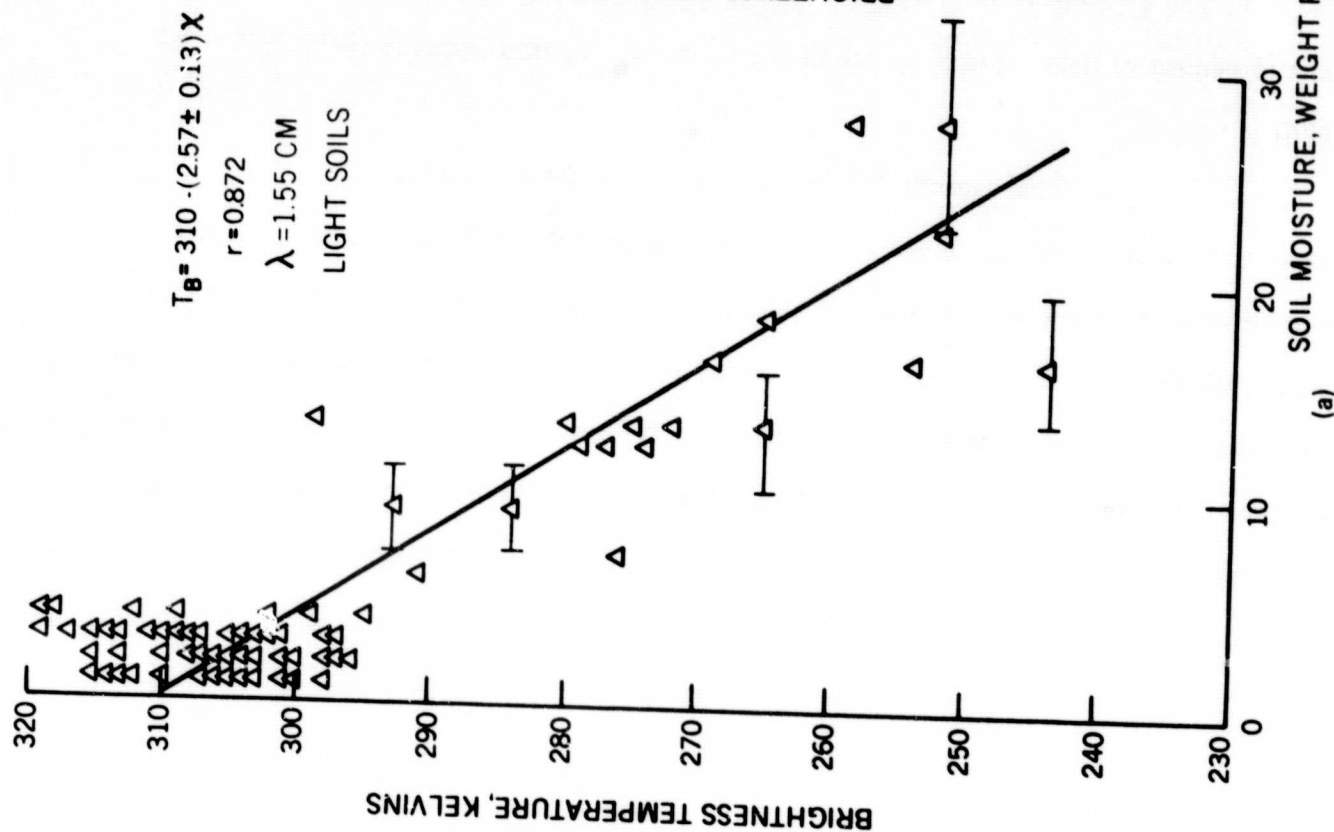
Figure 2(a,b). 19.35GH$_z$ (1.55 cm) Brightness Temperatures Versus Soil Moisture by Weight, Percent for Sandy and Clay Loam Soils in the 0 to 1 cm Soil Layer for March 7-13, 1972 Aircraft Flights over Phoenix, Arizona (Schmugge et al., 1976)

6
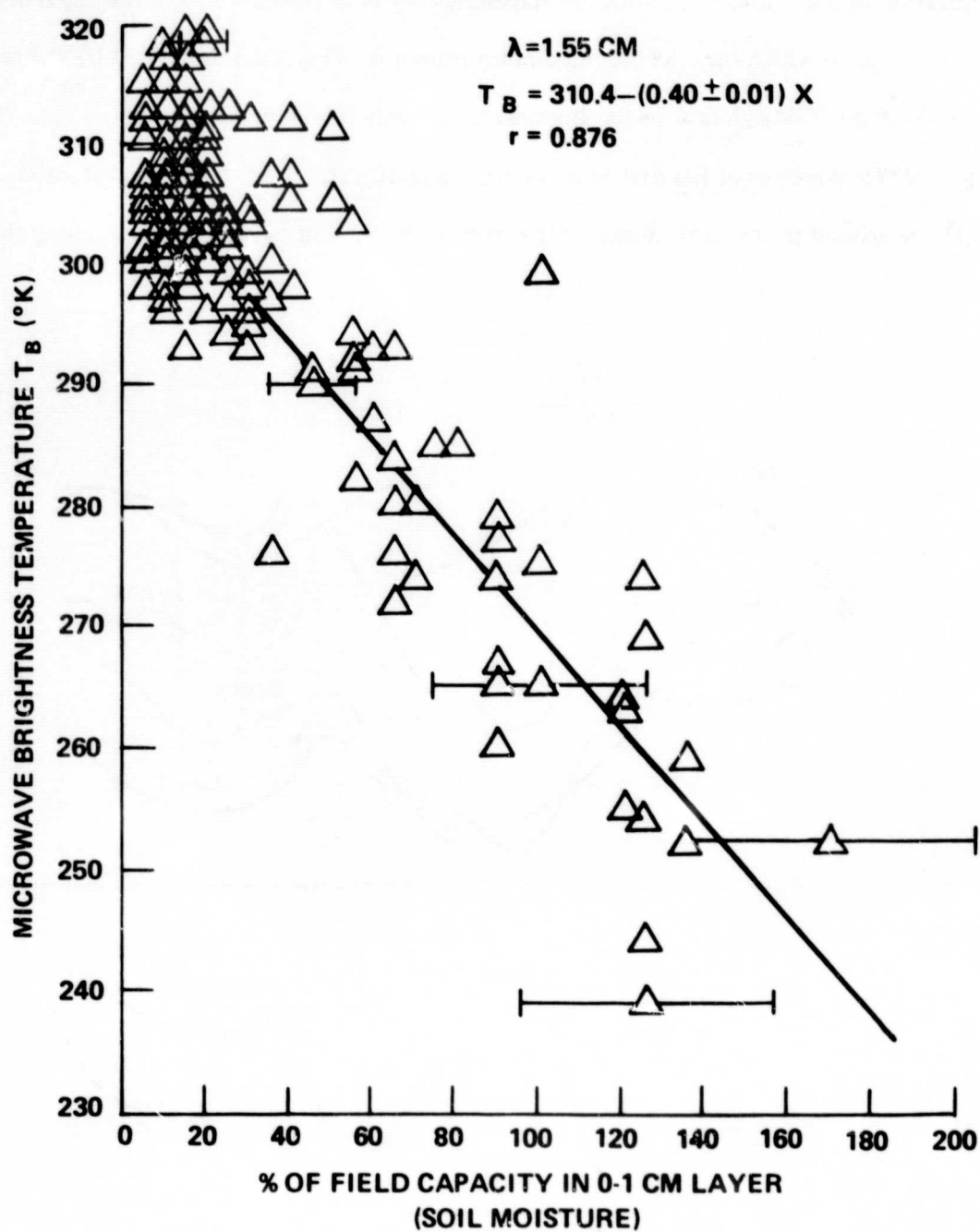
Figure 2(c). The Relationship Between Aircraft Observed Microwave Brightness Temperatures ($^\circ$K) at 19.35GH$_z$ and Soil Moisture, in Percent of Field Capacity, in the 0-1 cm Layer for Bare Agricultural Fields near Phoenix, Arizona (Schmugge et al., 1976)

7

Attempt to observe soil moisture variations from space have been frustrated by the coarse spatial resolution of the sensor (> 25km), the screening effects of vegetation, and the rapid drying of the surface layer to which the 1.55 cm radiometer responds. This is demonstrated by the results of the analysis of the ESMR data over the Illinois-Indiana area following heavy rains in June 1973 (Schmugge, 1977). Analysis of Landsat imagery for 9 and 10 June 1973 shows a substantial amount of bare ground in this area. Figure 3 is a plot of the T_B and rainfall variation along the
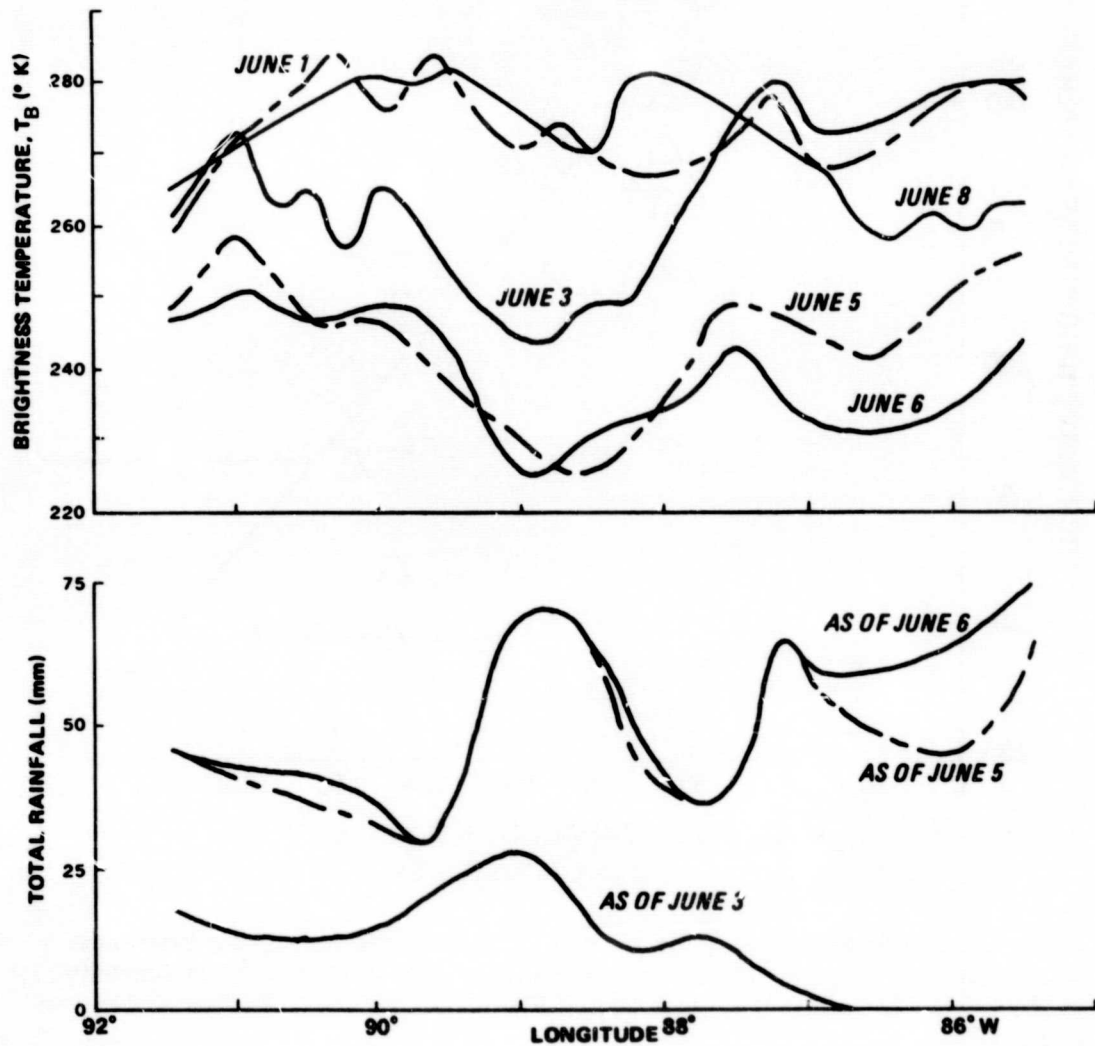
Figure 3. Variation of Nimbus 5 ESMR Brightness Temperature and Total Rainfall Along a Selected Latitude (40° N) Line for the Illinois-Indiana Area in June 1973

8

40°N latitude for 5 days earlier in the month. There is a 20-30°K decrease in T_B between 1 and 3 June in response to 25mm of rainfall at 89°W, while there was no decrease at 86°W where there was no rain. On 6 June the low T_B (< 230K) was noted for these areas receiving almost 75mm of rainfall. However two days later, 8 June, T_B has increased to the pre-rainfall values of 1 June. This indicates that the surface layer of the soil has dried significantly in this two day interval. During this period there was another area in the southern part of Illinois which received a similar amount of rain but for which T_B decreased by only 20-30°K. This is a winter wheat growing area and the Landsat imagery indicated a denser vegetation cover which screened the low T_B of the moist soils.

This screening effect of vegetation was also observed by Barton (1978) in the analysis of EMSR data over a test site at Deniliquin in southeast Australia. He found that the ESMR data did not indicate a soil moisture change following rains in October 1976, while ground measurements of soil moisture at a few points changed from 6 to 20% following the rain. The conclusion was that the 1.55 cm radiometer was not able to respond to soil moisture variations through a vegetative canopy which in this case was thick tufted grass 20 cm high.

An additional study was conducted over the northwest corner of Oklahoma using data from the fall of 1973 in order to determine the relationship between the Nimbus 5 ESMR T_B's and antecedent rainfall. Fig. 4 shows the good relationship found by McFarland and Blanchard, 1977, between Nimbus ESMR T_B values and Antecedent Precipitation Index (API) in inches, where:

$$API_{(i+1)} = K_i (P_i + API_i)$$

P_i = Precipitation on day 1 (limited to a maximum of 6.35 cm)

K_i = Dimensionless depletion constant for day 1

They found that Nimbus-5 ESMR data was responsive to variations in antecedent soil moisture in the near surface layer providing the target area was predominantly bare soil or low density vegetation cover.

9
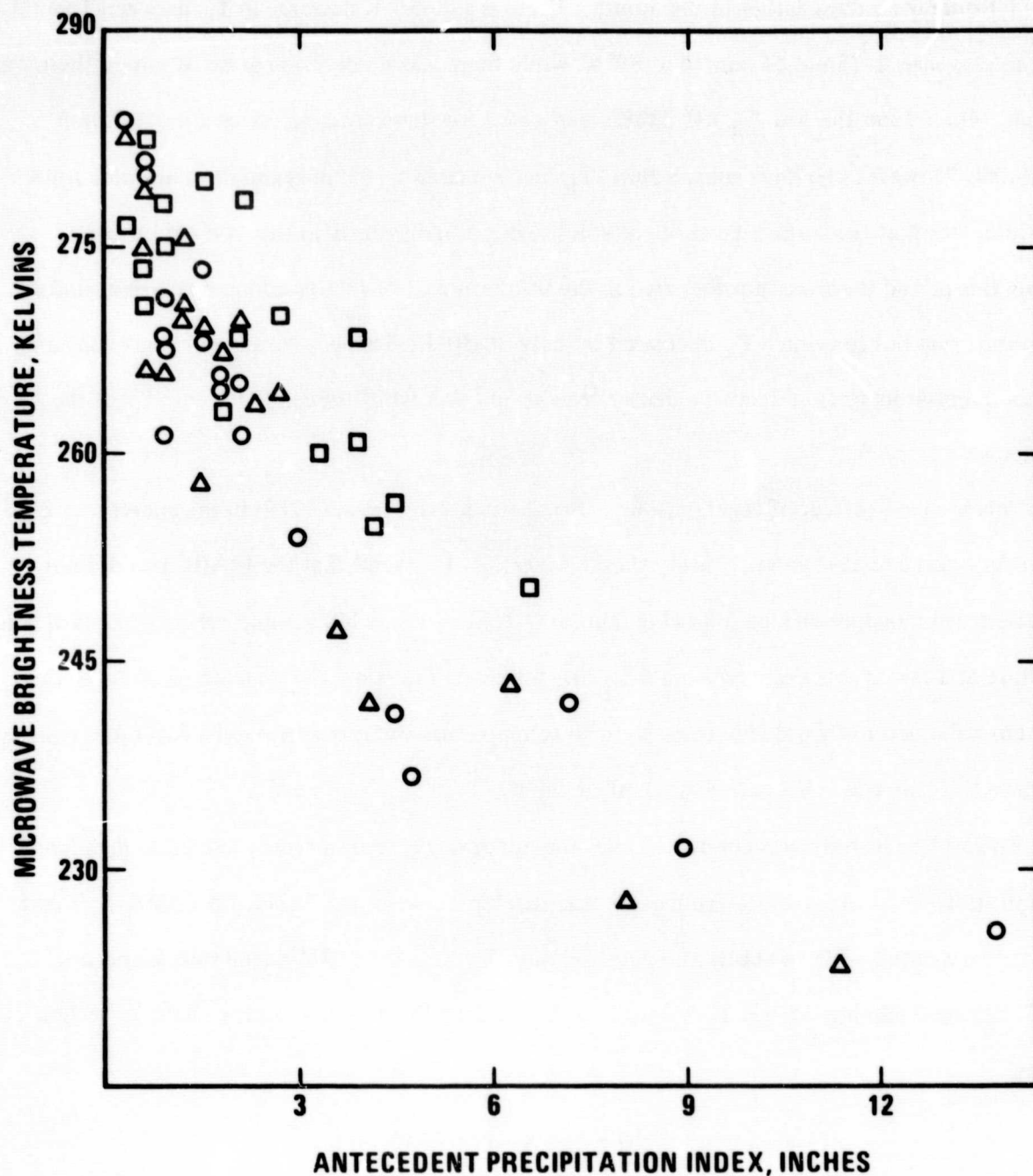
Figure 4. Nimbus–5 ESMR Brightness Temperatures (°K) Versus Antecedent Precipitation Index over Northwest Oklahoma. (McFarland and Blanchard, 1977)

These studies have indicated the sensitivity of spaceborne microwave radiometers to large scale moisture changes under certain conditions, i.e., with little or no vegetative canopy screening the soil. The results to be discussed in this paper are of persistent low values of T_B (< 250K)

10

observed over large areas of Australia during the first quarter of 1974. It is our conclusion that these lowered values of T_B resulted from large amounts of standing water or flooding in the radiometer field of view rather than simply wet soil.

4. THE 1974 EAST AUSTRALIAN FLOODS

A. Background Information

Figure 5 shows the annual mean rainfall in inches for Australia. The wetter areas are indicated by grey tones (>20 in.) and are located along the coastal strips to the north, northeast, east, southeast and southwest. During the summer months (December to February) the rainy intertropical zone of convergence (ITC) is indicated by a low pressure monsoonal area which forms over the north equatorial coast. Extensive extremely dry desert regions (<10 in. (250mm)/yr.) are shown

THE AUSTRALIAN ENVIRONMENT
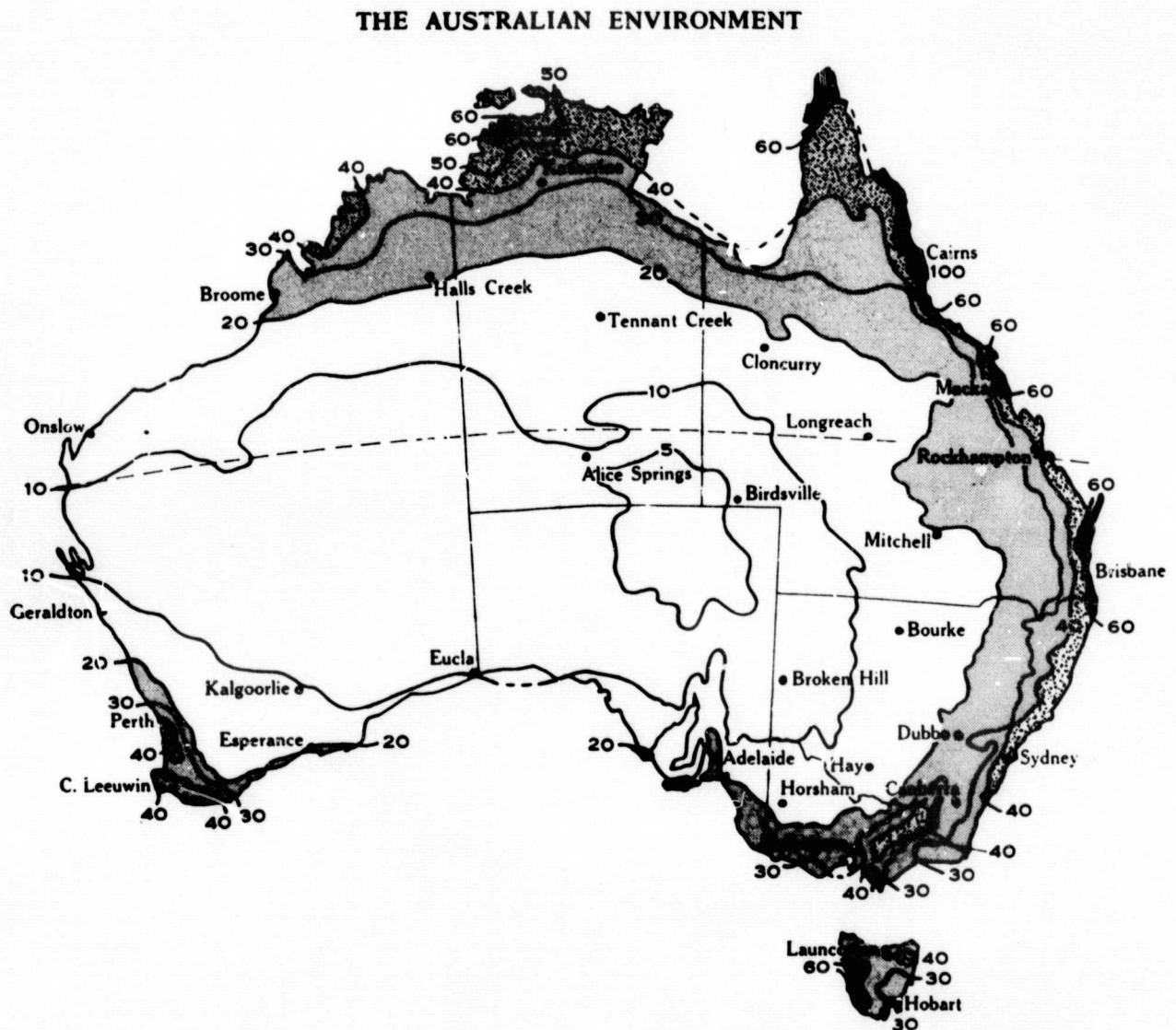
Figure 5. Annual Mean Rainfall (in.) (Leeper, 1973)

covering large areas of central and western Australia. Evaporation is high and on the average accounts for 87% of the rain as compared to 60% for Europe and North America. Thus only a small proportion of rainfall becomes surface runoff except during heavy rain periods. During the winter months, June to August, the north coast is dry as the ITC moves northward into the northern hemisphere while the southern coastal strips receive rain from the west-to-east travelling lows in the "Roaring Forties" (Leeper, 1973). Ten to twenty inches of rain per year falls in semiarid Queensland and New South Wales (with exception of coastal strips) and permit sheep and cattle grazing in vast treeless grasslands and low open hilly woodland, examples of which are shown in Fig. 6(a and b) (Laut et. al., 1977). A large number of deep artesian wells in the Great Artesian Basin (eastern quarter of Australia in the Central Basin) supplement the surface water supply for the sheep and cattle industries. Orographic maps of Australia indicate 1000 to greater than 3000 ft. (300 to 1000m) elevations exist in the eastern highlands, while the Central Basin is generally below 500 ft. This basin has two major drainage systems; the Lake Eyre interior drainage and the Murray-Darling River. These two gently sloped systems have less than 1 inch (2.5 cm) runoff annually. The typical sand dunes, erosion channels and claypans of the Lake Eyre region in south central Australia are shown in Fig. 6(c and d).

The lakes in the central internal drainage basin in south Australia are dry most of the time and only fill during periods of heavy rainfall. In 1974 it was possible to monitor their flooding with the Nimbus 5 ESMR. The particular lakes that will be discussed in some detail are: Bulloo Lake which is the terminal of the Bulloo River in southwestern Queensland and Lake Yamma Yamma with the neighboring lowlands of Cooper's Creek (Fig. 7).

The area of flooding that will be discussed is along the Darling River in New South Wales. Early in the period the flooding was concentrated around the town of Walgett in northeast section of New South Wales (Fig. 8). The flooded area will appear to move down river ending up at Menindee in March 1974.

The January to March 1974 period was an extremely anomalous season in that heavy rainfall and severe flooding occurred in the northern coastal plains of Queensland (south of the Gulf of

(b)

Gibber plain with tufted grasses

(d)

Dune with erosion remnants, and the lake in the background

(a)

Hill and stony plain with saltbush

(c)

Dunes, claypans and channels near Lake Eyre

Figure 6. Conventional Photographs Showing Terrain and Vegetation Features in New South Wales and South Australia. (Laut et al., 1977)

14
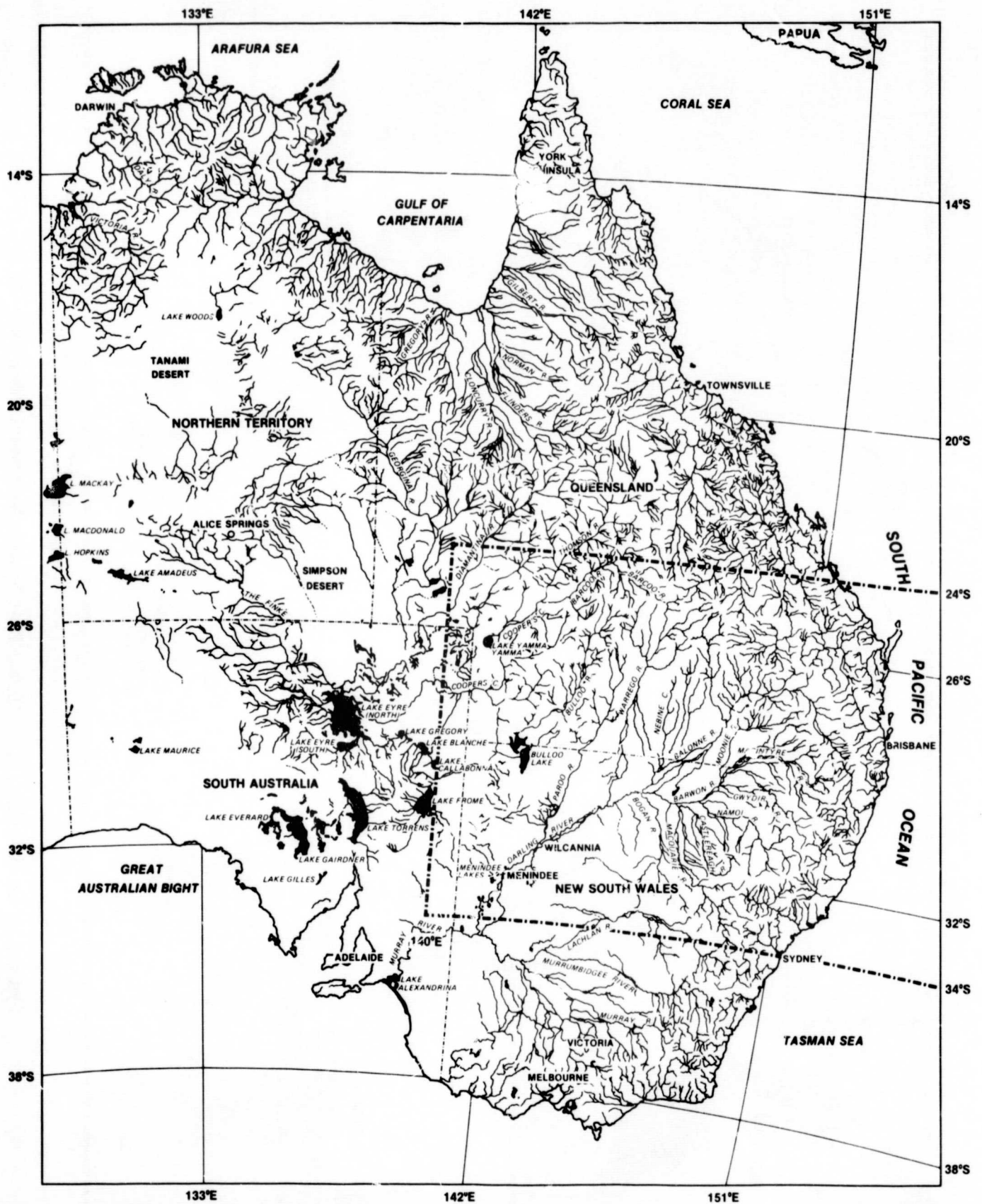
Figure 7. Major River Systems with Minor Tributaries and Lake Locations, Eastern Half of Australia, Dot-Dash Outlines the Study Area to be Analyzed in This Paper (Courtesy, Atlas of Australian Resources, 1956)
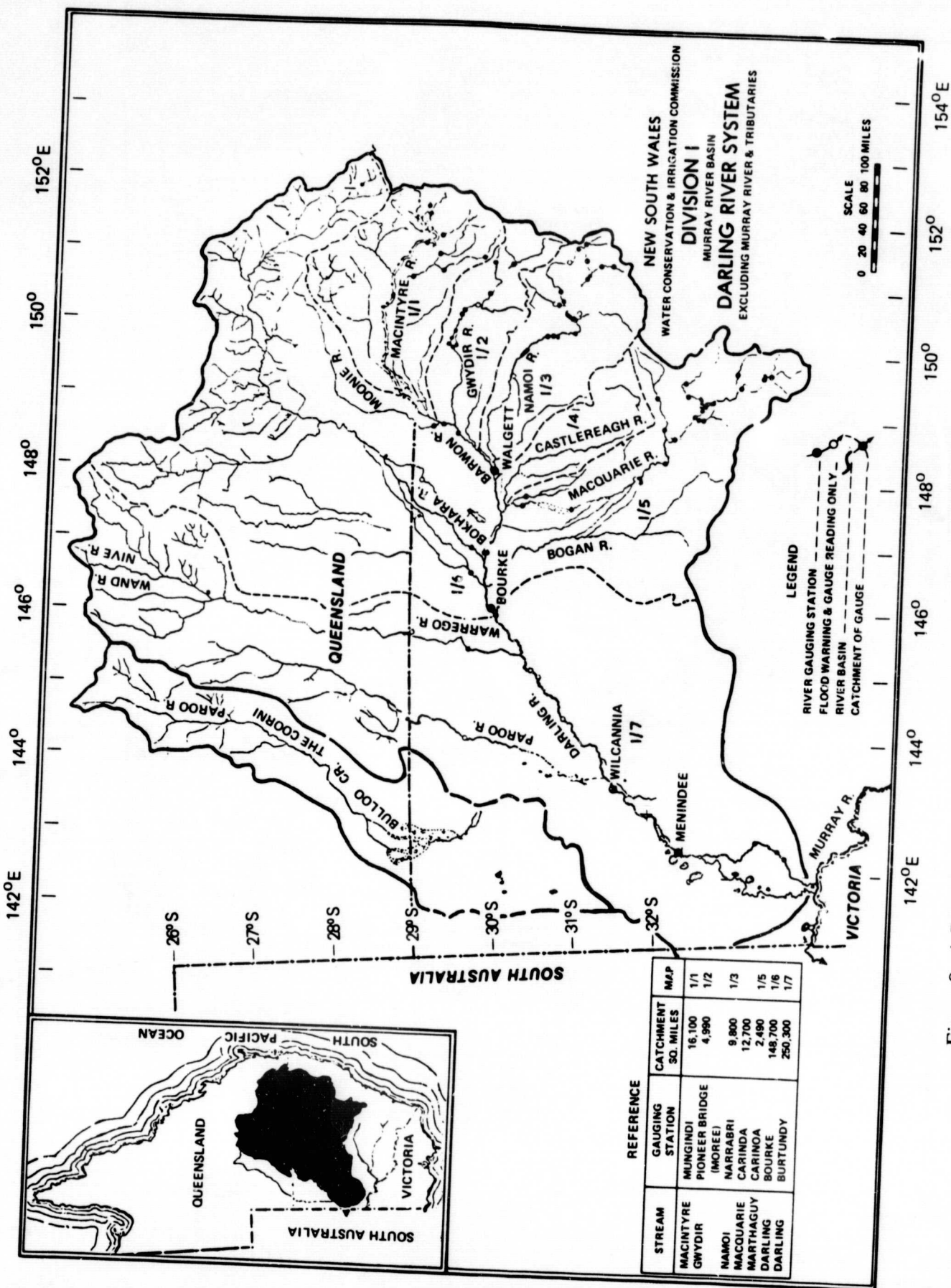
Figure 8. A Detailed Chart of the Darling River System, New South Wales, Australia

REFERENCE

STREAM	GAUGING STATION	CATCHMENT SQ. MILES	MAP
MACINTYRE	MUNGINDI	16,100	1/1
GWYDIR	PIONEER BRIDGE (MOREE)	4,990	1/2
NAMOI	NARRABRI	9,800	1/3
MACQUARIE	CARINDA	12,700	1/5
MARTHAGUY	CARINDA	2,490	1/6
DARLING	BOURKE	148,700	1/6
DARLING	BURTUNDY	250,300	1/7

LEGEND

RIVER GAUGING STATION
FLOOD WARNING & GAUGE READING ONLY
RIVER BASIN
CATCHMENT OF GAUGE

NEW SOUTH WALES
WATER CONSERVATION & IRRIGATION COMMISSION

DIVISION I
DARLING RIVER SYSTEM
MURRAY RIVER BASIN
EXCLUDING MURRAY RIVER & TRIBUTARIES

SCALE
0 20 40 60 80 100 MILES

Carpentaria, the Coopers Creek area of southwest Queensland, the Lakes Eyre, Frome, Gairdner, Torrens area in South Australia and the Darling River basin in New South Wales and south Queensland. Figure 9 shows the rainfall in both Queensland and New South Wales for January and February 1974 which ranged from 50 to 2000 percent of the normal 25 to 400mm/month (Monthly Weather Review, New South Wales, Queensland, 1974). The runoff due to this heavy rainfall flowed slowly southward through normally dry channels into a network of rivers which feed into Lake Eyre and the Darling River system (Warner, 1977). A similar flood occurred in Australia during the 1949-50 period in which large areas of the Lake Eyre drainage division were inundated and rivers flooded up to 30km in width in certain areas. Flooding in the lower reaches of this inland water systems can occur 3 months after the rainfall event in the headwaters of these drainage divisions. (Australian Water Resources Council, 1976, Gibbs and Maher, 1967, Pittock, 1975.)

In the last 100 years, the worst previous flood years in Australia occurred in 1852-3, 1863, 1870, 1875, 1887, 1889-94, 1909-11, 1916-17, 1921, 1925, 1931, 1934, 1949-50 (Foley, 1954).

B. Chronology of the 1974 Flood

At the beginning of January 1974 a normal summer monsoonal trough extended from the Gulf of Carpentaria southeastward through Queensland and northern New South Wales. By 9-10 January 1974, this surface trough became well defined and ensuing heavy rains (>300mm) fell in Queensland and New South Wales. In addition Tropical Storm Wanda moved westward inland over southeast Queensland and increased the anomalous rainfall (>200mm) from 24-26 January 1974. (Monthly Weather Review, NSW, 1974.) The Nimbus-5 ESMR photofacsimile pictures, Figure 10 (a,b), starting 9 January 1974 show the NW/SE oriented trough with white indicating "cold" brightness areas of rain and/or wet ground over a dark "warm" ground background. Ocean areas are white since they consist of colder T_B values due to low surface emissivities (0.4). Heavy rains (300mm from 7-10 Jan. at Walgett) fell on the upland portions of the Darling river watershed producing a large, almost circular region, of lowered T_B values seen in Figure 10(c to e). As the region dried out, the total area of lowered T_B decreased and began to move down to the south and take

17
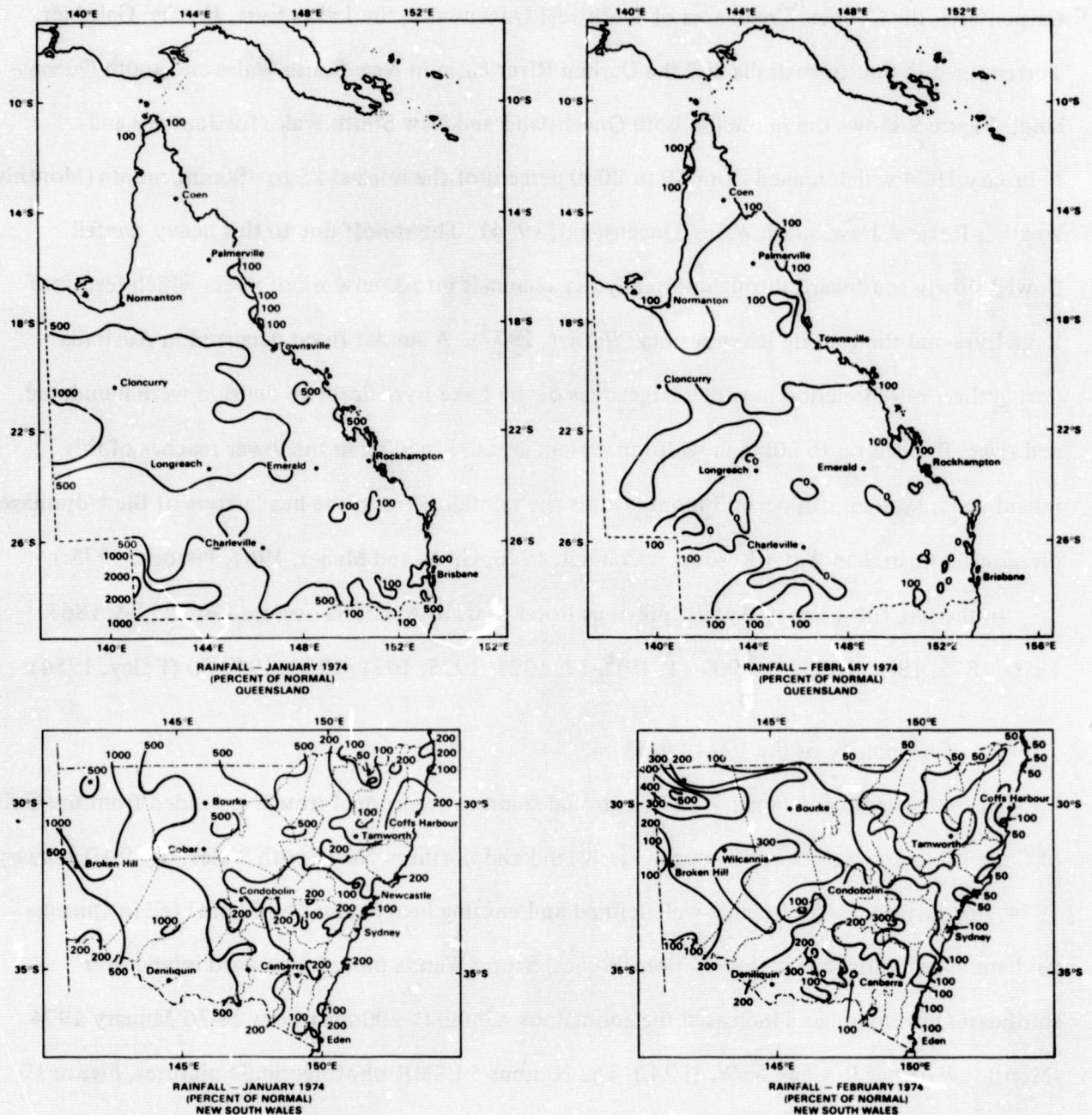
Figure 9.   Rainfall (in percent of normal) for January and February 1974,
Queensland and New South Wales

the shape of the lower portion of the drainage basin, Figure 10(f to j). Additional rain (35 to

62mm) of 19-20 February increased the size of the "cool" T_B region, Figure 10(k). The region

continued to move south and decrease in size until 21 March when the sequence stops, Figures 10

(l to p). To the west of the Darling River basin, the left side of Figure 10, are the interior lakes of

9 JAN. 1974
(NIGHT)
RAIN
(a)

10 JAN. 1974
(NIGHT)
RAIN
(b)

16 JAN. 1974
(DAY)
RAIN
(c)
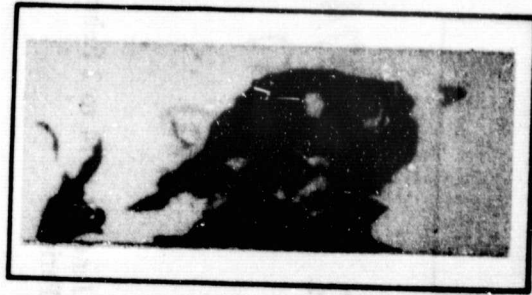
19 JAN. 1974
(NIGHT)
(d)

Figure 10(a to d). Nimbus–5 ESMR (19.35 GHz) Photofacsimile Pictures of the East Australian Floods from 9 January 1974 to 19 January 1974. The White Arrow Indicates the Wet Ground in the Darling River System During this Period.

21 JAN. 1974   24 JAN. 1974   31 JAN. 1974   2 FEB. 1974
(NIGHT)   (NIGHT)   (NIGHT)   (NIGHT)
(e)   (f)   (g)   (h)

Figure 10(e to h). Nimbus–5 ESMR (19.35 GH$_z$) Photofacsimile Pictures of the East Australian Floods from 21 January 1974 to 2 February 1974. The White Arrow Indicates the Wet Ground in the Darling River System During this Period.
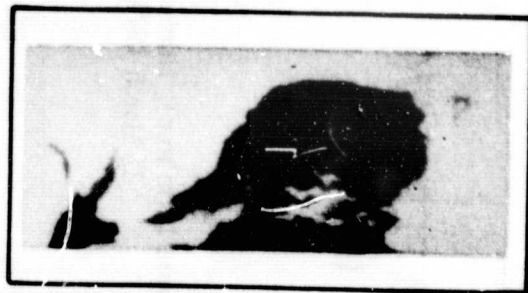
7 FEB. 1974   14 FEB. 1974   19 FEB. 1974   23 FEB. 1974
(NIGHT)   (NIGHT)   (NIGHT)   (NIGHT)
                                RAIN
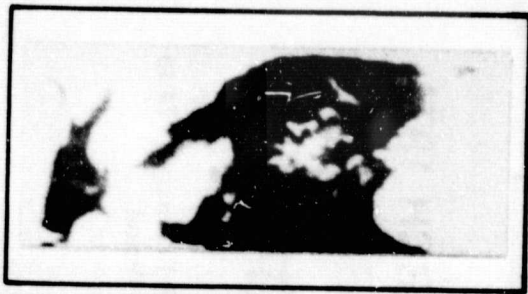
(i)   (j)   (k)   (l)

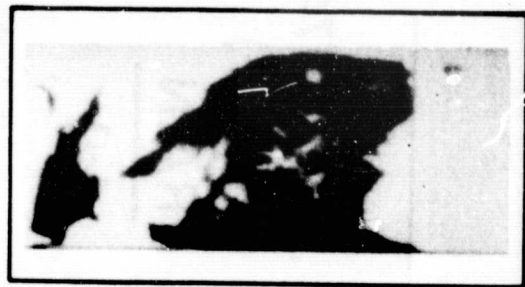Figure 10(i to l).   Nimbus–5 ESMR (19.35 GHz) Photofacsimile Pictures of the East Australian Floods from 7 February 1974 to 23 February 1974.   The White Arrow indicates the Wet Ground in the Darling River System During this Period.

21

28 FEB. 1974   5 MARCH 1974   14 MARCH 1974   21 MARCH 1974
(NIGHT)   (NIGHT)   (NIGHT)   (NIGHT)

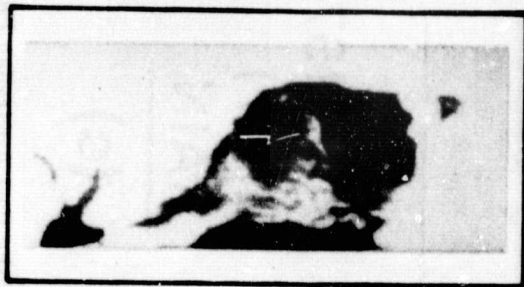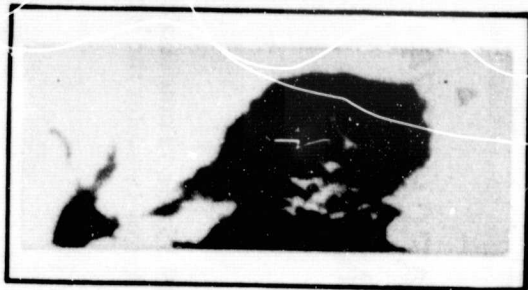(m)   (n)   (o)   (p)

Figure 10(m to p). Nimbus–5 ESMR (19.35 GH$_z$) Photofacsimile Pictures of the East Australian Floods from 28 February 1974 to 21 March 1974. The White Arrow Indicates the Wet Ground in the Darling River System During this Period.

22

South Australia. These lakes show a large change in size from 9 January to 23 February as the runoff from the uplands drain into these interior basins.

A more quantitative presentation of these features is given in Figure 11 which contains contour maps of brightness temperature values for the Darling River basin. Regions with $T_B < 240°K$ for night orbits and $T_B < 250°K$ for day orbits are shaded or ziptoned to indicate regions with substantial flooding. This is based on the assumption that areas with persistent low brightness values are those having a substantial amount of standing water within the sensor field of view. The results presented earlier over Illinois in 1973 (Schmugge et al., 1977) and Australia in 1976 (Barton, 1978) indicate that wet soils alone would not produce the persistent low T_B values. The particular values of T_B chosen to delineate areas with substantial flooding were those which would indicate that 25-30% of the area within the sensor's field of view were water covered. This percentage was determined by observing that the T_B of unflooded grassland was 280°K while the lowest T_B observed for the interior lakes were in the 170 to 180°K range. Thus for a day pass

$$\text{Percent of standing water} = \frac{T_B \text{ (dry)} - T_B}{T_B \text{ (dry)} - T_B \text{ (wet)}} = \frac{280°K - T_B}{280°K - 180°K}$$

It is recognized that this is only an estimate and that regions with temporarily saturated soils could also have T_B's in the 250°K range.

Figure 11 shows the T_B contour map for the time of the most intense rainfall over the area with extensive ground wetness. The low T_B values are the result of increased ground wetness rather than being due to the rain itself since the lowest T_B expected for intense rain is approximately 250°K (Wilheit et al., 1977). By 22 January (Figure 11b) the shaded area has decreased to 150 x 200 km section centered around the town of Walgett. The other shaded area north of the town of Wilcannia is Lake Bulloo, an internal drainage basin, Above that is Lake Yamma Yamma and the Cooper Creek lowland is apparently just beginning to fill with water. The shaded area around Walgett continues to shrink on 24 January while Lake Bulloo and Lake Yamma Yamma-Cooper Creek areas continue to grow and intensify. Additional rains on 25 and 26 January (18mm
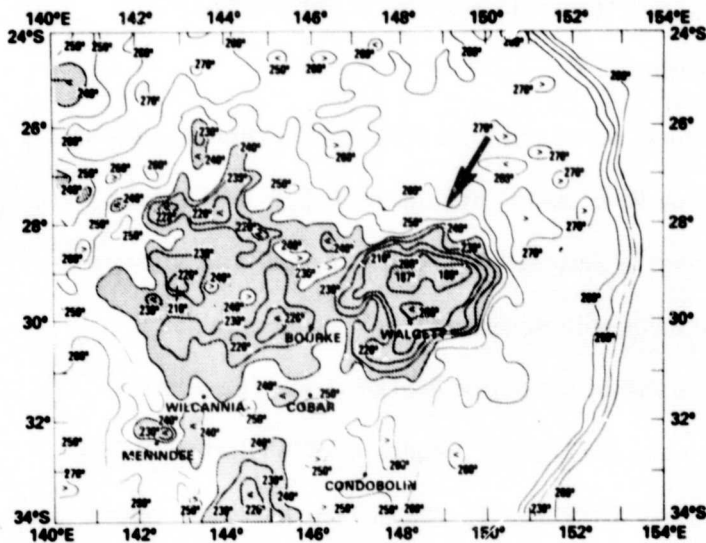
NIMBUS 5 ESMR (19.35 GHz)
10 JANUARY 1974 ORBIT 5306 (NIGHT-RAIN)

(a)
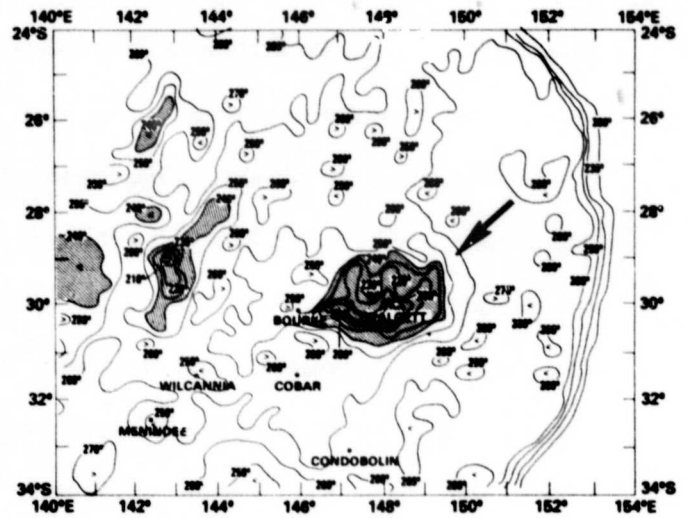
NIMBUS 5 ESMR (19.35 GHz)
22 JANUARY 1974 ORBIT 5467 (NIGHT)

(b)
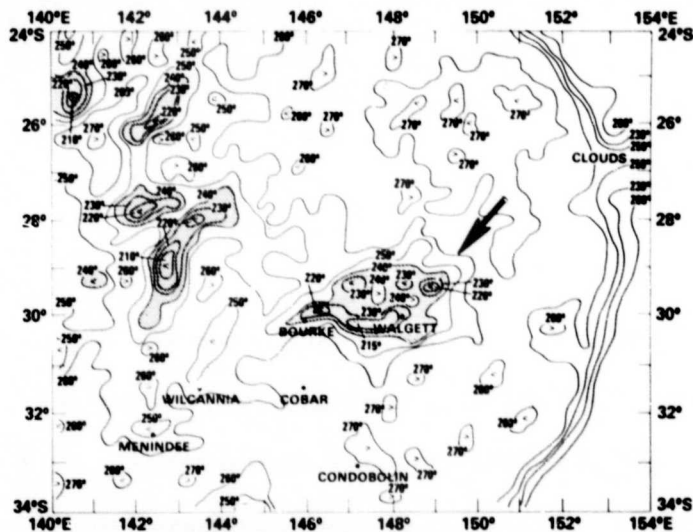
NIMBUS 5 ESMR (19.35 GHz)
24 JANUARY 1974 ORBIT 5494 (NIGHT)

(c)
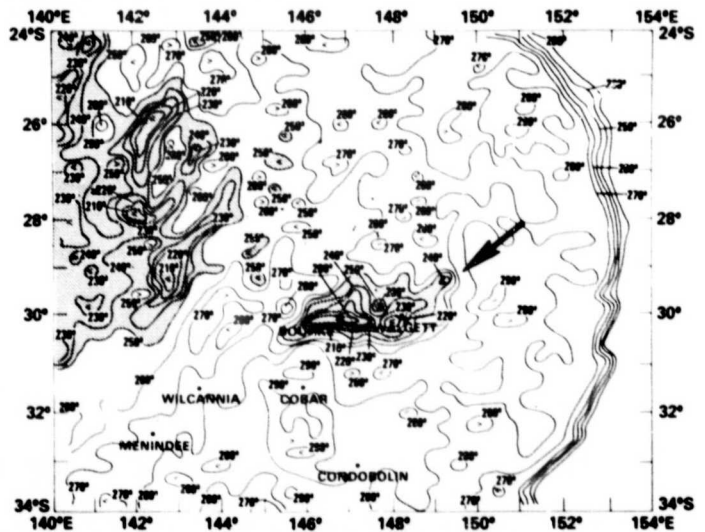
NIMBUS 5 ESMR (19.35 GHz)
30 JANUARY 1974 ORBIT 5568 (DAY)

(d)

Figure 11(a,d). Nimbus-5 ESMR (19.35GH$_z$) Grid-Print Maps of Brightness Temperatures, (T_B, °K) (1¾2.5 Million Mercator). The Single Arrow Indicates the flooded Darling River System. The Double Arrow Indicates the Lake Yamma Yamma and Flooded Coopers Creek Area, 10 January to 30 January 1974
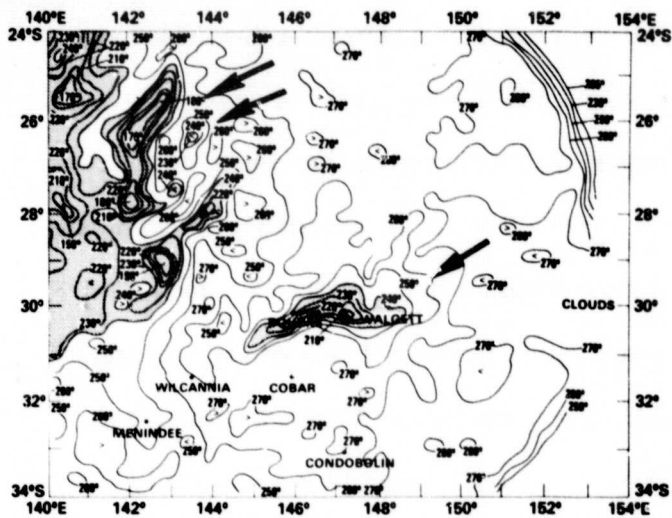
NIMBUS 5 ESMR (19.35 GHz)
2 FEBRUARY 1974 ORBIT 5615 (NIGHT)

(e)
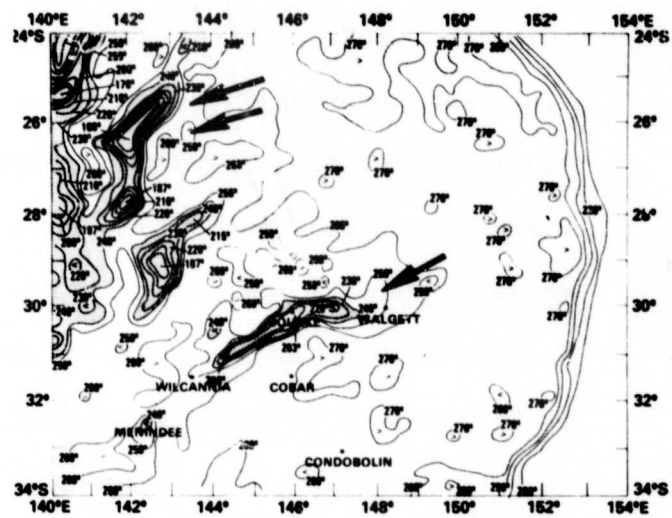
NIMBUS 5 ESMR (19.35 GHz)
7 FEBRUARY 1974 ORBIT 5682 (NIGHT)

(f)
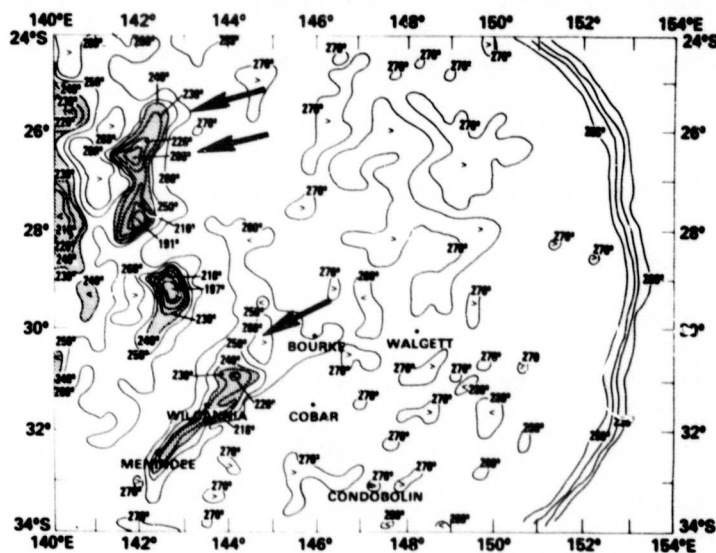
NIMBUS 5 ESMR (19.35 GHz)
5 MARCH 1974 ORBIT 6031 (NIGHT)

(g)
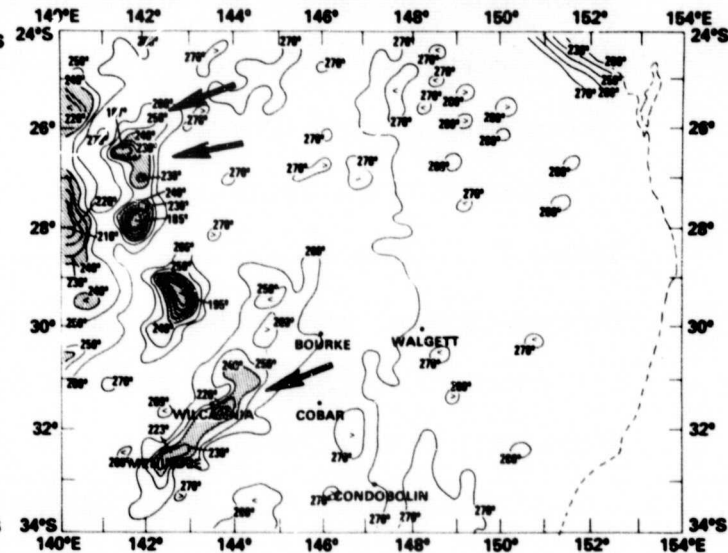
NIMBUS 5 ESMR (19.35 GHz)
14 MARCH 1974 ORBIT 6152 (NIGHT)

(h)

Figure 11(e,h). Nimbus-5 ESMR (19.35 GH$_z$) Grid-Print Maps of Brightness Temperatures,
(T$_B$, °K) (1:2.5 Million Mercator). The Single Arrow Indicates the flooded Darling River System.
The Double Arrow Indicates the Lake Yamma Yamma and Flooded Coopers Creek Area,
2 February to 14 March 1974

25

at Walgett), produced little change in the 30 January map of the Darling River basin except for the movement of the shaded area to the southwest. There was a substantial increase in the shaded area for the lake regions where heavier rains had fallen. The 2 and 7 February 1974 maps show the continued shrinkage of the shaded area in the Darling River basin and the movement of the flooded area to the southwest. The leading edge moved from 70 km to approximately 30 km northwest of the town of Wilcannia during this interval or about 8 km per day. In each case, the lowest T_B was $210°K$ or less indicating at least 50 to 60% water within the field of view of the radiometer. The two lakes in the northwestern portion of this analysis have become well defined with T_B's as low as $170°K$, indicated by the double arrows in Figures 11(e to h). Figure 12 is a Landsat 1 (MSS-7) image of the same area on 6 February 1974 when waters in the Barcoo River channels overflowed into Lake Yamma Yamma and Coopers Creek lowlands reaching a maximum width of 60 km. The flood boundaries are readily mapable because of large differences in surface reflectance between the dark flooded area and the lighter dry uplands (Robinove, 1978, Short et al., 1976). From this image, the total extent of the flooded area is estimated to be 160 km by 50 km which is in reasonable agreement with the area within the $180°K$ countour line in Figure 11f.

The 5 and 14 March maps indicate the continued movement of the shaded southwest down the Darling River, with the lowering of T_B becoming less intense, i.e., the minimum is now about $220°K$. Similarly the shaded region of the lakes has also shrunk.

A hydrograph (Figure 13) for the Barwon River at Walgett, provided by the New South Wales Water Resources Commission, was compared with the values of T_B for a 50 km x 50 km area around the town of Walgett. Generally, the low T_B values relate well to the river gage height which is an indicator of the overbank flow. In particular, the peak of gage height occurs on 17 January, slightly prior to the minimum value of $T_B = 184°K$, on 19 January 1974. This value indicates that 80 to 90% of this 50 x 50 km area was flooded. The subsequent rise of T_B corresponds well to the decrease in gage height. A photograph of the flooding at the Dangar Bridge, Walgett on 17 January 1974 is shown in Figure 14.
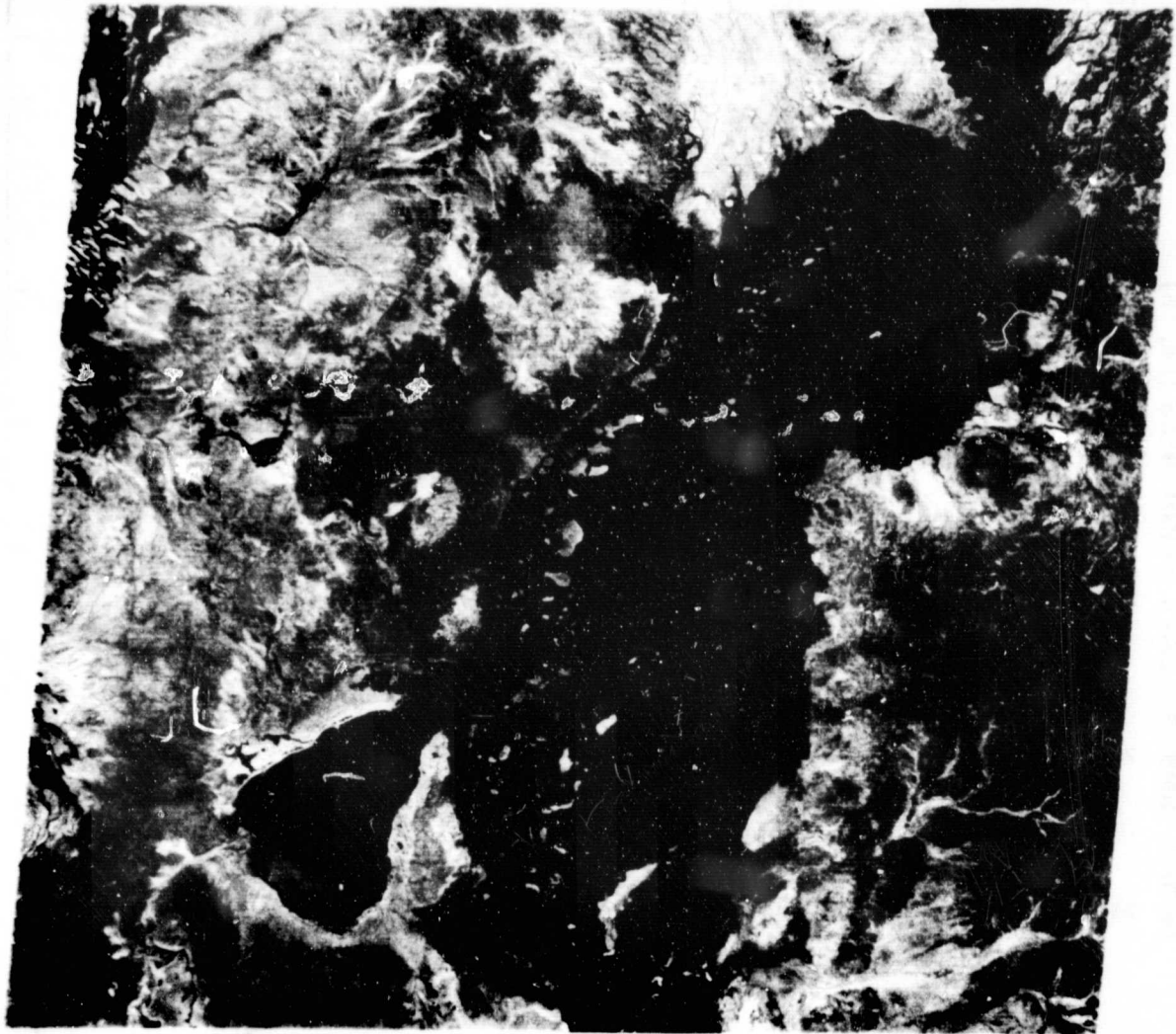
Figure 12. Landsat 1 (MSS–7, Frame No. 1563–23530) Recorded on 6 February 1974. **Lake Yamma** Yamma (Appendage Lower Left) is Shown Near Darker flooded Coopers Creek Low-lands, (Center Right)

An initial attempt was made to measure the flooded area from the Nimbus 5 ESMR grid print maps of brightness temperatures. Six regions which were covered by T_B value $<240°$K, night and $<250°$K, day were planemetered (Figure 15). The daily integrated changes for area 6 along the Darling River basin is shown in Figure 16(a). Starting at zero before the rains of 9 to 11 January,
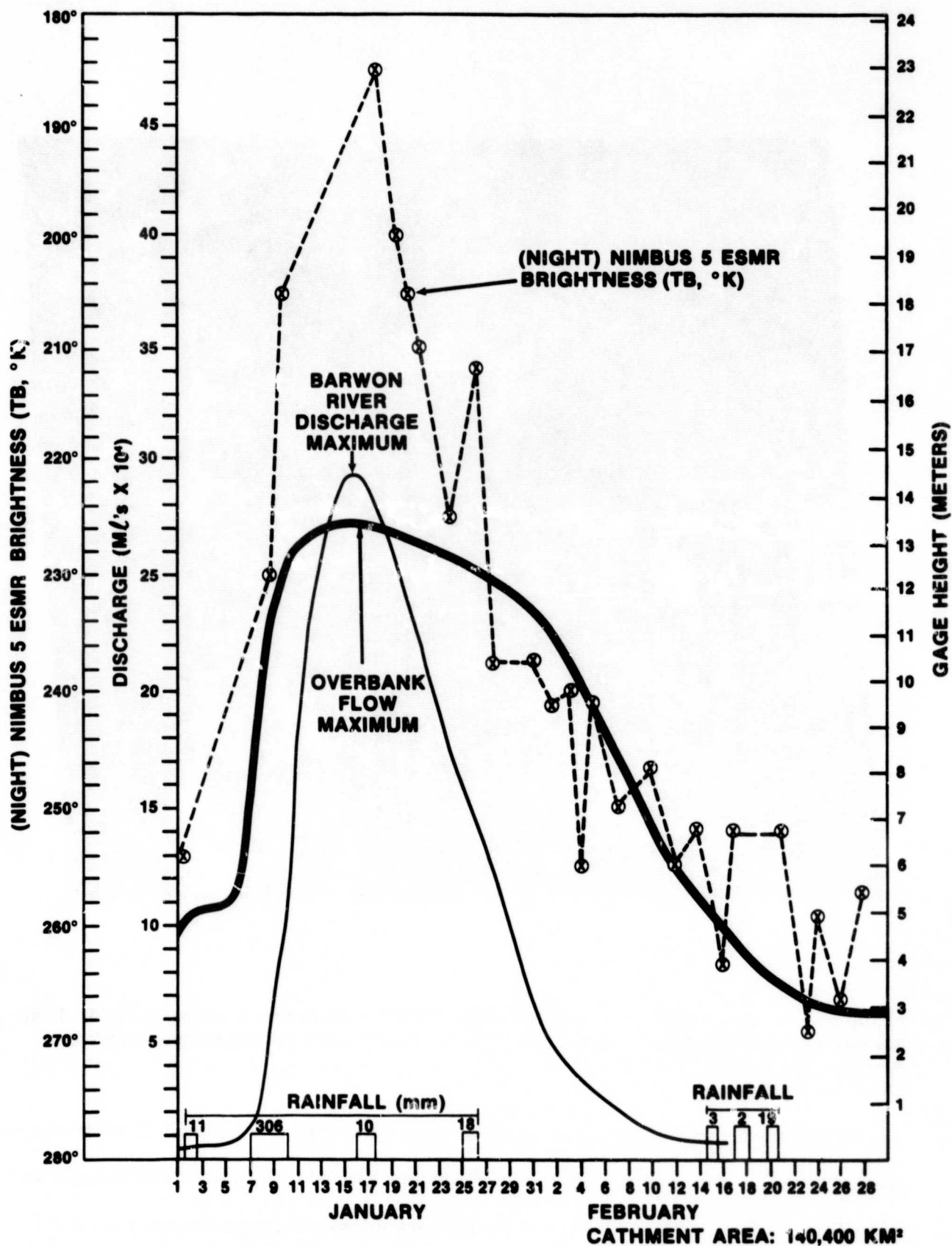
Figure 13. Barwon River at Walgett, New South Wales, 1974 Flood Hydrograph and Superimposed Nimbus-5 night ESMR Brightness Temperatures (T_B, °K) and Daily Rainfall (mm)

28
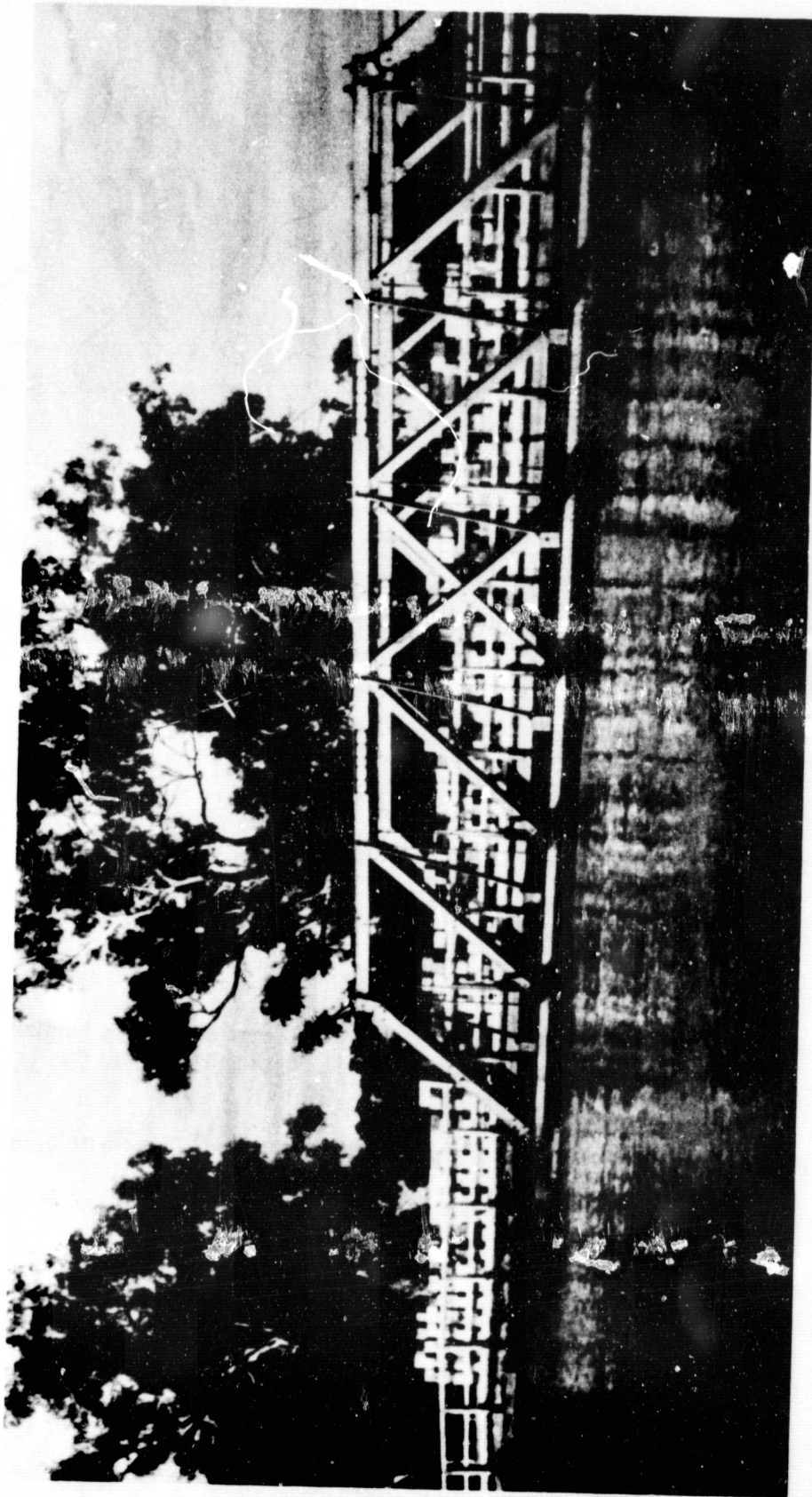
Figure 14. Photograph of Maximum Flooding on 17 January 1974 at the Dangar Bridge, Walgett, New South Wales

Figure 15. Six Regions in Eastern Australia which were covered by Nimbus-5 ESMR Brightness Temperatures, <240° K, Night and <250° K, Day

it reaches a peak on 10 January which probably includes a substantial area with bare wet soils. By 15 January, these surface soils have dried out and the area reduces to a value of 50 to 60,000 km² and the area continues to decrease with the exception of sharp spikes resulting from rains in late January and mid February 1974. Recall that the shaded areas contained at least 20-30% standing water, therefore, the actual flooded area will be somewhat less than that indicated in Figure 16(a). Figure 16(b) shows the daily integrated flooded area changes for all areas 1 to 6. One major flood k occurred on 30 January 1974 while minor peaks occurred on 10, 18 January, 20 February and
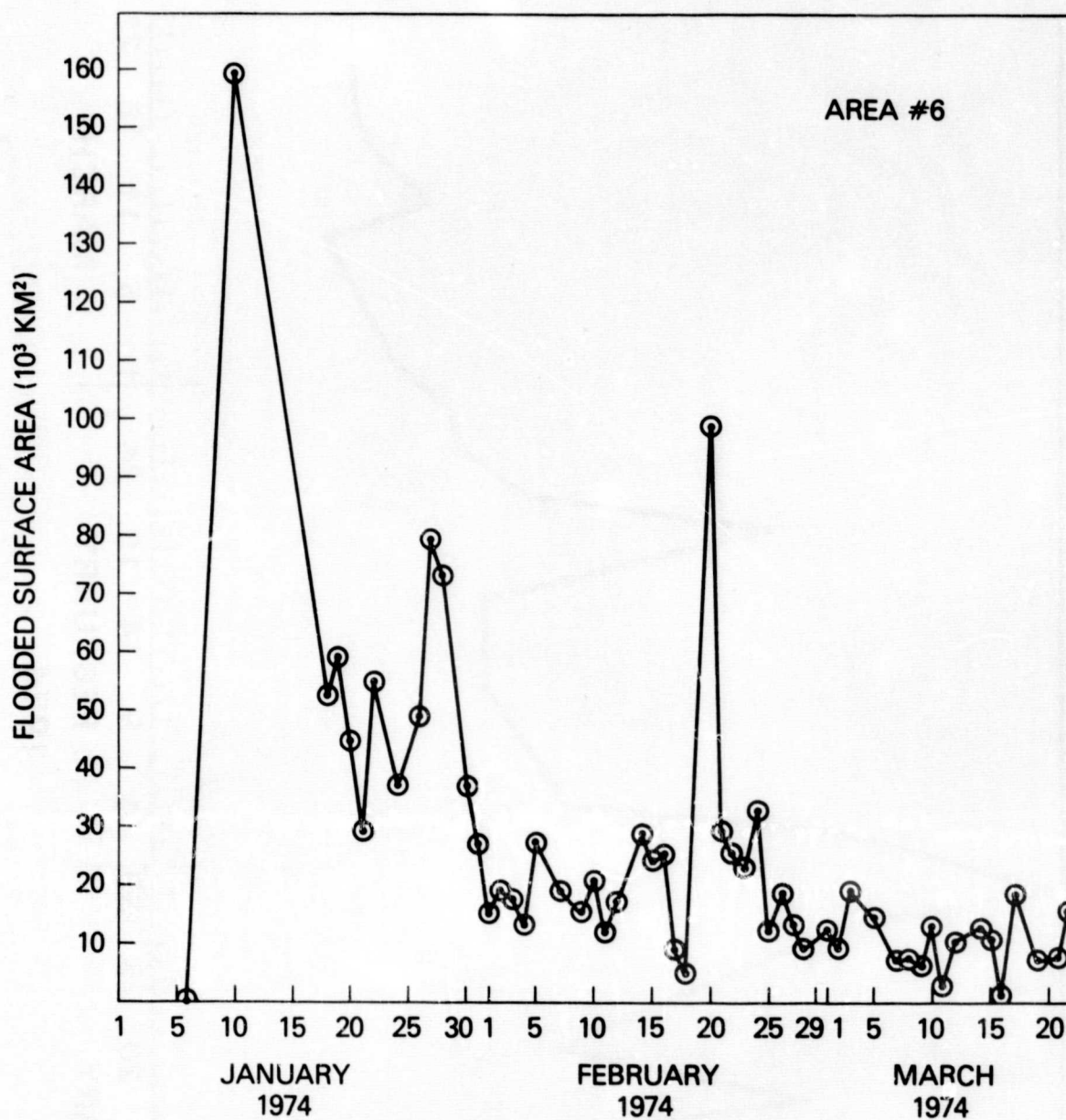
Figure 16(a). Estimated total Flooded Surface Area (km² for Area Six Shown in Figure 15, in Eastern Australia from January to March 1974 Derived from Nimbus-5 ESMR (19.35 GH$_z$ Data (Day: T_B = 240° K and <, Night: T_B = 240° K and <)

11 March 1974. Color pictures of the near-flood area maximum on 1 February and near-minimum on 11 March 1974 are shown on the frontispiece of this study. A more complete description of the wet season flooding in the South Carpentaria Plains (Area 2) may be found in a paper by Simpson and Doutch, 1977.

Figure 16(b). Estimated Total Flooded Surface Area (km²) for the Six Regions Shown in Figure 15, in Eastern Australia from Jan. to March 1974 Derived from Nimbus–5 ESMR (19.35GH$_z$) Data (Day: T$_B$ = 250°K and <, Night: T$_B$ = 240°K and <)
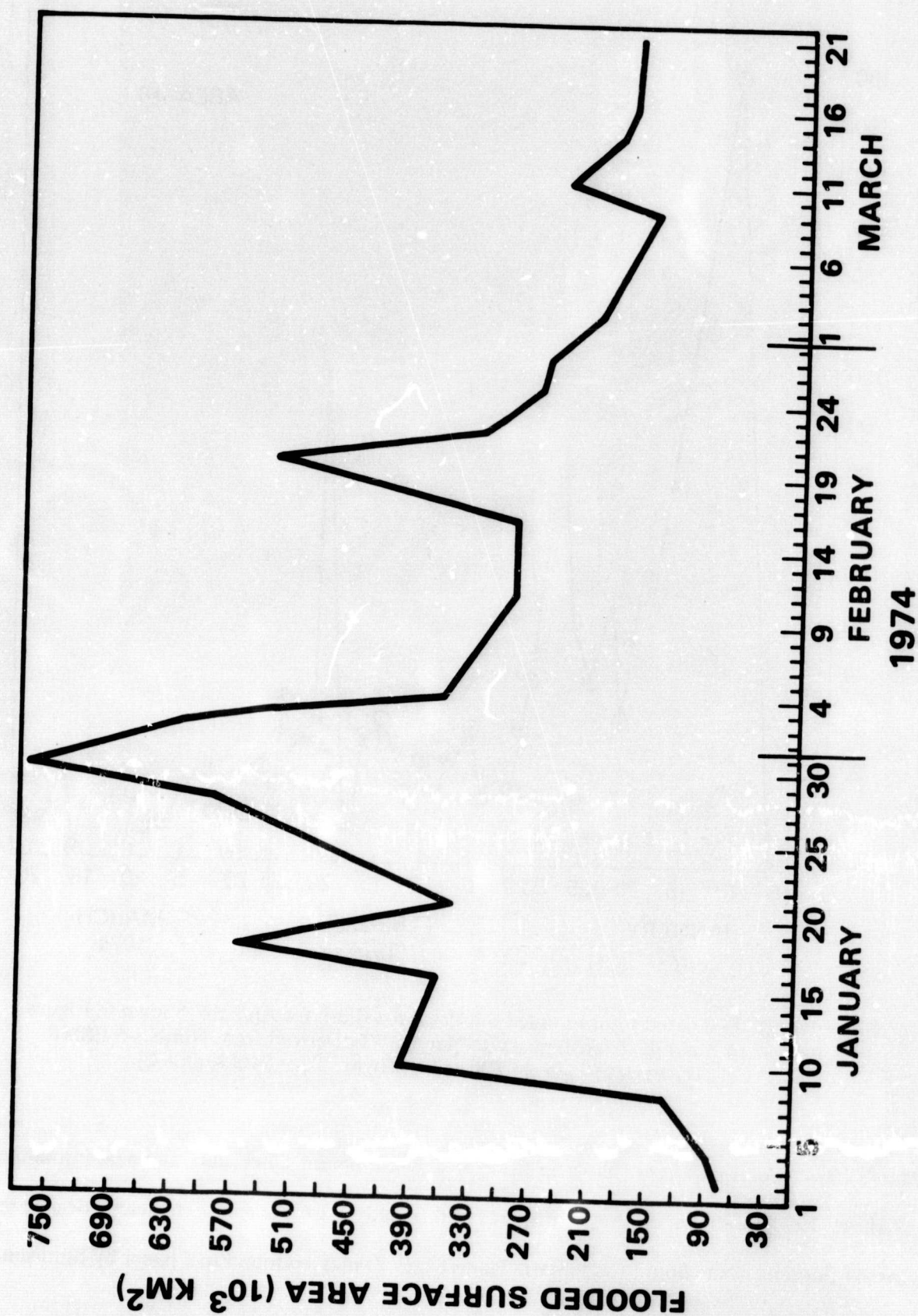
32

5. CONCLUSIONS

The passive microwave brightness temperature observations of the Nimbus-5 ESMR were used to detect and monitor the development of flooded areas in the Darling River basin of New South Wales, Australia. This capability was based on the observation of areas of persistent lowered values of T_B which were attributed to the presence of flooded areas or standing water within the ESMR field of view. In the Darling River basin, the temporal variation of both size and location was monitored through the first quarter of 1974. The area with substantial flooding varied in size from approximately 60,000 km^2 immediately following the heavy rains in mid-January to about 10,000 km^2 in late March 1974. Its center moved approximately 600 km from town of Walgett to half-way between the town of Wilcannia and Menindee and it changed in shape from roughly circular to oblong as it moved down stream. The motion is believed to be that of the flood waters since there were no anomalously large rains over the downstream portion of basin following the heavy rains early in January 1974.

These results indicate that microwave brightness temperature observations are another useful tool for monitoring surface water. This satellite capability will be considerably enhanced when improved spatial resolution becomes available in the future. Longer wavelength sensors will also provide greater sensitivity to soil moisture and standing water and less sensitivity to vegetation cover. Examples of this are shown in the results of Eagleman and Lin (1976) from the Skylab 21cm radiometer data in which soil moisture changes were monitored through crop cover present in the U.S. Great Plains area.

REFERENCES

Adler, R. F. and E. B. Rodgers, 1977: Satellite-observed latent heat release in a tropical cyclone, Monthly Weather Review, Vol. 105, pp. 956-963.

Allison, L. J., E. B. Rodgers, T. T. Wilheit and R. W. Fett, 1974: Tropical cyclone rainfall as measured by the Nimbus 5 electrically scanning microwave radiometer, Bull. Amer. Meteor. Soc.; 55. pp. 1074-1089.

Allison, L. J., 1975: A multisensor analysis of Nimbus 5 data recorded on January 22, 1973, NASA TN D-7911, Goddard Space Flight Center, Greenbelt, Md. p. 41.

Allison, L. J., 1977: Geological applications of Nimbus radiation data in the middle east, NASA TN D-8469 Goddard Space Flight Center, Greenbelt, Md. p. 79.

Atlas of Australian Resources, 1956: Conservation of surface water, Dept. of National Development, Canberra, p. 12.

Austin, P. M. and S. G. Geotis, 1978: Evaluation of the quality of precipitation data from a satellite-borne radiometer, Final Report, NASA Grant NSG 5024 Dept. of Meteorology, MIT, Cambridge, Mass. 02139, p. 32.

Australian Water Resources Council, 1976: Review of Australia's water resources, 1975, Department of Natural Resources, Australian Gov't Publishing Service, Canberra, Australia p. 170.

Barton, I. J., 1978: A case study comparison of microwave radiometer measurements over bare and vegetated surfaces, JGR, Vol. 83, No. B7, pp. 3513-3517.

Cihlar, J. and F. T. Ulaby, 1974: Dielectric properties of soils as a function of moisture content, RSL Tech. report 177–47, University of Kansas Center for Research, Lawrence, Kansas, p. 61.

Eagleman, J. R. and W. C. Lin, 1976: Remote Sensing of Soil Moisture by a 21cm Passive Radiometer, JGR, Vol 81, pp. 3660-3666.

Foley, J. C., 1954: The climate of Australia, atlas of Australian resources, Climate Regions, Dept. of National Development, Canberra, Australia p. 16.

Gibbs, W. J. and J. V. Maher, 1967: Rainfall deciles as drought indicators, Bull. No., 48, Bureau of Meteorology, Melbourne, Australia p. 117.

34

Kidder, S. Q., 1976: Tropical oceanic precipitation frequency from Nimbus 5 microwave data, Atmos. Science Paper 248, Colorado State University, Ft. Collins, Colorado, p. 50.

Kidder, S. Q. and T. H. Vonder Haar, 1977: Seasonal oceanic precipitation frequencies from Nimbus 5 microwave data, Jrl. of Geophysical Res., Vol. 82, No. 15, pp. 2083-2086.

Laut, P., G. Keig, M. Lazarides, E. Loffler, C. Margules, R. M. Scott, and M. E. Sullivan, 1977: Environments of south Australia, Province 8, Northern Arid, CSIRO, Canberra, Australia, p. 254.

Leeper, G. W. ed., 1973: The Australian environment, Commonwealth Scientific and Industrial Research Organization (CSIRO), Melbourne University Press, Australia, p. 163.

McFarland, M. J. and B. J. Blanchard, 1977: Temporal correlation of antecedent precipitation with Nimbus 5 ESMR brightness temperatures, Preprints of 2nd Hydrometeorology Conference, Toronto, Canada, American Meteorological Society, pp. 311-315.

Meneely, J. M., 1975: Application of the Nimbus 5 ESMR to rainfall detection over land surfaces, Final Report E/S No. 1008, Earth Satellite Corp., Washington, DC, p. 48.

Monthly Weather Review, 1974: New South Wales and Queensland, Department of Science, Bureau of Meteorology, Australia, January and February, p. 24.

Moore, R. K., L. J. Chastant, L. J. Porcello, J. Stevenson and F. T. Ulaby, 1975: Microwave remote sensors, Manual of Remote Sensing, Vol. 1, American Society of Photogrammetry, Falls Church, Va., pp. 499-534.

Newton, R. W., 1977: Microwave Remote Sensing and Its Application to Soil Moisture Detection, Tech. Report RSC-81 Texas A&M University, College Station, Texas, p. 500.

Nordberg, W., J. Conaway, D. B. Ross, and T. Wilheit, 1971: Measurements of Microwave Emission from a Foam-Covered, Wind-Driven Sea, JAS, Vol. 28, pp. 429-435.

Oberste-Lehn, 1970: Phenomena and properties of geologic materials affecting microwaves, a review, Stanford Remote Sensing Laboratory, TR 70-10, Stanford University, Stanford, California, p. 57.

Otterman, J., P. D. Lowman and V. V. Salomonson, 1976: Surveying earth resources by remote sensing from satellites, Geophysical Surveys, 2, D. Reidel Publishing Co.. Holland, pp. 431-467.

Pittock, A. B., 1975: Climate change and the patterns of variations in Australian rainfall, Search, Vol. 6, No. 11-12, pp. 498-504.

Poe, G., A. Stogryn and A. T. Edgerton, 1971: Determination of soil moisture content using microwave radiometry, Final Report No. 1684, FR-1 for Dept. of Commerce, Contract No. 0-35239, Aerojet Electrosystems Co., Azusa, CA, 91702.

Rango, A. and A. T. Anderson, 1974: Flood hazard studies in the Mississippi river basin using remote sensing, Water Resources Bulletin, Vol. 10, No. 5, American Water Resources Assn., pp. 1060-1081.

Rango, A. and V. V. Salomonson, 1974: Regional flood mapping from space, Water Resources Research, Vol. 10, No. 3, pp. 473-484.

Rao, M. S. V., W. V. Abbott and J. S. Theon, 1976: Satellite-derived global oceanic rainfall atlas, NASA SP-410, National Aeronautics and Space Administration, Washington, DC.

Robinove, C. J., 1978: Interpretation of a landsat image of an unusual flood phenomenon in Australia, Remote Sensing of Envir. 7, pp. 219-225.

Rodgers, E. H., Siddalingaiah, A. T. C. Chang and T. Wilheit, 1978: A statistical technique for determining rainfall over land employing Niimbus 6 ESMR measurements, Third Conf., on Atmospheric Radiation, June 28-30, 1978, Davis, CA, pp. 126-129.

Savage, R. C. and J. A. Weinman, 1975: Preliminary calculations of the upwelling radiance from rain clouds at 37.0 and 19.35GHz, Bull. Amer. Meteorol. Soc., 56, pp. 1272-1274.

Schmugge, T. J., A. Rango, L. J. Allison, and T. T. Wilheit, 1974 (a): Hydroiogic applications of Nimbus 5 ESMR data, NASA X-910-74-51, Goddard Space Flight Center, Greenbelt, Md. p. 21.

Schmugge, T. J., P. Gloersen, T. T. Wilheit and F. Geiger, 1974. (b): Remote sensing of soil moisture with microwave radiometers, Jrl. of Geoph. Res., 79 (2), pp. 317-325.

Schmugge, T. J., T. Wilheit, W. Webster and P. Gloersen, 1976: Remote sensing of soil moisture with microwave radiometers—II NASA TN-D-8321, Goddard Space Flight Center, Greenbelt, Md., p. 34.

Schmugge, T. J., J. M. Meneely, A. Rango and R. Neff, 1977: Satellite microwave observations of soil moisture variations, Water Resources Bulletin, Vol. 13, No. 2, pp. 265-281.

Short, N. M., P. D. Lowman, S. C. Freden and W. A. Finch, 1976: Mission to earth, Landsat views the world, NASA SP-360, National Aeronautics and Space Admininistration, Wash. D.C., pp. 422-423.

Simpson, C. J. and H. F. Doutch, 1977: The 1974 wet season flooding in the southern Carpentaria plains, Northwest Queensland, BMR Jrl. of Australian Geology and Geophysics, 2, pp, 43-51.

Stout, J. E. and D. W. Martin, 1979: Estimating rain with geosynchronous satellite images, (submitted to MWR)

Ulaby, F. T., 1977: Microwave remote sensing of hydrologic parameters, Proceeding of the Eleventh International Symposium on Remote Sensing of Environment, Vol. 1, April 25-29, 1977, ERIM, Ann Arbor, Michigan, pp. 67-86.

Vickers, R. S. and G. C. Rose, 1971: The use of complex dielectric constant as a diagnostic tool for the remote sensing of terrestrial materials, AFCRL-71-0438, Colorado State University, Ft. Collins, Colorado, p. 39.

Warner, R. F., 1977: Hydrology, Chapter 3, Australia, a geography, D. N. Jeans, ed., St. Martin's Press New York, p. 571.

Weinman, J. A. and P. J. Guetter, 1977: Detection of rainfall distribution from microwave radiation measured by the Nimbus 6 ESMR, J. App. Met., 16, pp. 437-442.

Wiesnet, D. R., D. F. McGinnis and J. A. Pritchard, 1974: Mapping of the 1973 Mississippi river floods by the NOAA-2 satellite, Water Resources Bulletin, vol. 10, No. 5, American Water Resources Assn., pp. 1040-1049.

Wilheit, T. T., 1972: The electrically scanning microwave radiometer (ESMR) experiment. Nimbus 5 Users Guide, NASA Goddard Space Flight Center, Greenbelt, Md., pp. 55-105.

Wilheit, T. T., J. Theon, W. Shenk, L. J. Allison and E. Rodgers, 1973: Meteorological interpretations of the images from Nimbus 5 electrically scanning microwave radiometer, J. Appl., Meteor., 15, pp. 168-172.

Wilheit, T. T., 1973: ESMR corrections to the user's guide, Nimbus 5 Data Catalog, Vol. 3., Goddard Space Flight Center, Greenbelt, Md., pp. 5-4 to 5-6.

Wilheit, T. T., A. T. C. Chang, M. S. V. Rao, E. B. Rodgers and J. S. Theon, 1977: A satellite technique for quantitatively mapping rainfall rates over the ocean, J. Appl. Meteor., 16, 5, pp. 551-560.

Zwally, H. J. and P. Gloersen, 1977: Passive microwave images of the polar regions and research applications, Polar Record, Vol. 18, No. 116, pp. 431-450.